Early Antiretroviral Therapy Preserves Functional Follicular Helper T and HIV-Specific B Cells in the Gut Mucosa of HIV-1-Infected Individuals

Cyril Planchais, Laurent Hocqueloux, Clara Ibanez, Sébastien Gallien, Christiane Copie, Mathieu Surénaud, Ayrin Kök, Valerie Lorin, Mathieu Fusaro, Marie-Hélène Delfau-Larue, et al.

Early antiretroviral therapy preserves functional follicular T Helper and HIV-specific B cells in the gut mucosa of HIV-1 infected individuals

Cyril Planchais[1,2], Laurent Hocqueloux[3], Clara Ibanez[1,2], Sébastien Gallien[2,4], Christiane Copie[5,6], Mathieu Surenaud[1,2], Ayrin Kök[7,8], Valérie Lorin[7,8], Mathieu Fusaro[11], Marie-Hélène Delfau-Larue[11], Laurent Lefrou[9], Thierry Prazuck[3], Michael Lévy[10], Nabila Seddiki[1,2], Jean-Daniel Lelièvre[1,2,4], Hugo Mouquet[2,7,8], Yves Lévy[1,2,4*], Sophie Hüe[1,2,11*]

[1] INSERM U955, Team 16, Université Paris Est Créteil, Faculté de Médecine, Créteil, F-94010, France

[2]Vaccine Research Institute (VRI), Université Paris Est Créteil, Faculté de Médecine, 94010, Créteil, France

[3]Service des Maladies Infectieuses et Tropicales, CHR d'Orléans-La Source, France

[4] Assistance Publique-Hôpitaux de Paris (AP-HP), Groupe Henri-Mondor Albert-Chenevier, Service d'immunologie clinique, Créteil, France

[5] Assistance Publique-Hôpitaux de Paris (AP-HP), Groupe Henri-Mondor Albert-Chenevier, Département de Pathologie, Créteil, France

[6]INSERM U955, Team 9, Université Paris Est Créteil, Faculté de Médecine, Créteil, F-94010, France

[7]Laboratory of Humoral Response to Pathogens, Department of Immunology, Institut Pasteur,

[8]INSERM U1222, Paris, 75015, France.

[9]Service d'Hépato-Gastro-Entérologie, CHR d'Orléans-La Source, Orléans

[10] Assistance Publique-Hôpitaux de Paris (AP-HP), Groupe Henri-Mondor Albert-Chenevier, Service d'Hépato-Gastro-Entérologie, Créteil, France

[11] Assistance Publique-Hôpitaux de Paris (AP-HP), Groupe Henri-Mondor Albert-Chenevier, Service d'immunologie biologique, Créteil, France

***Correspondence should be addressed to** Yves Lévy (yves.levy@aphp.fr) and Sophie Hüe (sophie.hue@aphp.fr), CHU Henri Mondor, 94010 Créteil, FRANCE

Phone: +33 149 812 298; Fax: +33 149 812 897.

Key words: HIV, gut homeostasis, early antiretroviral therapy, B cells, T_{FH} cells

Conflict of interest: The authors have declared that no conflict of interest exists.

ABSTRACT

Human immunodeficiency virus-1 (HIV-1) infection is associated with B-cell dysregulation and dysfunction. In HIV-1-infected patients, we previously reported preservation of intestinal lymphoid structures and dendritic-cell maturation pathways after early combination antiretroviral therapy (e-ART), started during the acute phase of the infection, compared with late cART (l-ART) started during the chronic phase. Here, we investigated whether the timing of cART initiation was associated with the development of the HIV-1-specific humoral response in the gut. The results showed that e-ART was associated with higher frequencies of functional resting memory B cells in the gut. These frequencies correlated strongly with those of follicular helper T-cells (T_{FH}) in the gut. Importantly, frequencies of HIV-1 Env gp140-reactive B cells were higher in patients given e-ART, in whom gp140-reactive IgG production by mucosal B cells increased after stimulation. Moreover, IL-21 release by peripheral-blood mononuclear cells stimulated with HIV-1 peptide pools was greater with e-ART than with L-ART. Thus, early treatment initiation helps to maintain HIV-1-reactive memory B cells in the gut, as well as T_{FH} cells, whose role is crucial in the development of potent affinity-matured and broadly neutralizing antibodies.

INTRODUCTION

Natural immunity to many viral diseases involves either circulating neutralizing antibodies produced by long-lived plasma cells in the bone marrow or the production of neutralizing antibodies by memory B cells reactivated by the infecting pathogen, frequently many years after the first exposure. For the HIV, however, the natural immune response appears ineffective (1). Among HIV-1-infected individuals, about 20% develop high titers of cross-reactive neutralizing antibodies to various regions of the HIV-1 envelope protein. In a few of these patients, known as elite neutralizers (about 1% of HIV-1-positive individuals), the cross-reactive antibodies include broadly neutralizing antibodies (bNAbs) capable of neutralizing most of the known HIV-1 strains (2). Unusual characteristics of bNAbs include high frequencies of V(D)J mutations, significantly extended third complementarity determining regions in the heavy-chain variable region (CDRH3), and polyreactivity and/or autoreactivity with human lipids and proteins (3).

The affinity-maturation process leading to the generation and selection of bNAb-expressing B cells remains poorly understood but must occur in germinal centers (GCs). Data from animal models demonstrate a critical role for follicular helper T-cells (T_{FH}) in the induction of GCs needed for the development of a high-affinity, pathogen-specific antibody response (4). The T_{FH} cells are targeted by the HIV-1 very early after infection and constitute a major cellular compartment for HIV-1 replication and viral particle production in the lymph nodes of viremic individuals (5). Despite their high susceptibility to HIV-1 infection, many studies have shown abnormal T_{FH} cell accumulation in HIV-1-infected patients compared to uninfected individuals (6). Interestingly, T_{FH} cell frequencies correlate positively with plasma viremia levels, and T_{FH} cell accumulation diminishes with combination antiretroviral therapy (cART) (6). Circulating T_{FH} cells were recently identified as a memory compartment of tissue-resident T_{FH} cells and were shown to share with these an ability to produce IL-21 and

provide helper signals to B cells (7). Therefore, T_{FH} function must be preserved to achieve efficient HIV-specific B-cell responses. T_{FH} cells isolated from lymph nodes of HIV-1-infected individuals do not provide adequate B-cell help *in vitro* (8). One of the complex mechanisms involved in T_{FH} cell dysfunction concerns the regulatory protein programmed death 1 (PD1). PD1 blockade has been shown to reinvigorate exhausted T cells (9). Incidentally, the PD1 ligand (PD-L1) has been described as highly expressed at the surface of B cells and dendritic cells in HIV-1-infected individuals (10, 11).

Previous studies have shown significant blood B-cell abnormalities in HIV-1-infected patients including an imbalance among peripheral mature B-cell subsets, with overexpression of tissue-like and activated memory B-cell subsets (12). HIV-associated exhaustion of tissue-like memory (TLM) B cells has been described based on a range of features and on similarities with T-cell exhaustion (13). These features include increased expression of multiple inhibitory receptors and weak proliferative and effector responses to various stimuli. Chronic immune activation appears to play a critical role in phenotypic and functional B-cell exhaustion. Conversely, resting memory (RM) B cells, which induce efficient secondary humoral responses, are depleted in the blood during the chronic stage of HIV-1 infection. When initiated at the chronic stage, cART fails to restore normal counts of blood memory B cells (14). In contrast, starting cART at the early stage of HIV-1 infection was associated with better restoration of RM B cells, in terms of both phenotype and function, as measured by the memory B-cell response to a recall antigen (15). Low RM B-cell counts may contribute to poor vaccine responses and weakened serological memory in HIV-1-infected individuals (16).

We previously reported that cART initiation during the early phase of HIV-1 infection (e-ART) ensured preservation of the mucosal gut lymphoid follicles (17). The tertiary lymphoid structures (TLSs) that develop during chronic inflammation can activate the molecular machinery needed to sustain *in situ* antibody diversification, isotype switching, B-

cell differentiation, and oligoclonal expansion, in keeping with their ability to function as active ectopic GCs. These observations raise the question of whether the timing of cART initiation may affect the development of the anti-HIV-1 humoral response in the gut. We designed a study to investigate this possibility.

The objective of this study was to compare e-ART to cART started later (l-ART), during the chronic stage of the infection, in terms of frequency, function, and specificity of mucosal T_{FH} and B cells in the gut mucosa of HIV-1-infected individuals. We compared peripheral blood mononuclear cells (PBMCs) and rectal biopsies from patients identified retrospectively after several years of e-ART or l-ART. Frequencies of functional T_{FH} and RM Env gp140-specific B cells in the gut mucosa were higher in the e-ART group. This finding supports a heretofore unsuspected role for the gut in generating antibodies against HIV-1.

METHODS

Study participants

Paired PBMCs and rectal biopsies were collected from 22 HIV-1-infected individuals who had been taking effective cART for several years. This treatment was started within 4 months after the diagnosis of primary HIV-1 infection in 9 patients (early cART, e-ART group) and later on, i.e., during the chronic stage of HIV-1 infection (Fiebig stage VI) (18), in 13 patients (late cART, l-ART group). The diagnosis of primary HIV-1 infection was defined as a negative or weakly positive ELISA with no more than four bands by Western blot and positive viremia and/or positive HIV-1 ELISA following a negative ELISA within the preceding 3 months. Gut biopsies from 6 HIV-1-seronegative individuals were included as controls. All rectal biopsies (~ 2 μm^3 each) were collected from the same site, 10-15 cm from the anal margin, to avoid potential bias due to regional variations among participants. **Table 1** reports the main features of the HIV-1-infected patients.

Ethics statements

All study participants provided written informed consent to participation in the study. This study was approved by our local ethics committee (Tours, France) (Comité de Protection des Personnes de Tours, 17th of December 2014, number: 2011-R26 (2011-CHRO-2011-02)

HIV-1 envelope glycoproteins (HIV-1 Env gp)

The recombinant HIV-1 Env YU-2 gp120 protein (gp120) and unlabeled HIV-1 and biotinylated YU-2 gp140 proteins (gp140 and gp140-biotin, respectively) were produced and purified as previously described (19, 20). Purified recombinant HIV-1 MN gp41 was provided by the NIH AIDS Reagent Program.

Cell isolation from rectal biopsies

Rectal biopsies were collected by rectoscopy at the regional hospital center in Orléans, France. Intraepithelial lymphocytes and lamina propria lymphocytes were obtained as previously described (17). Cells were used without further processing for immunophenotyping, ELISpot, and/or cell culture.

PBMC stimulation and chemokine assays

PBMCs ($5 \cdot 10^5$) were incubated for 6 days at 37 °C in a final volume of 300 µL of complete RPMI medium (Gibco) supplemented with 10% human AB serum in 96 deep well plates (Greiner MasterBlock, Sigma-Aldrich), with or without stimulation by pools of 150 HIV-1 15mer Gag or Env peptides (1 µg/mL, JPT, Berlin, Germany). *Staphylococcus aureus* enterotoxin B superantigen (SEB, 50 ng/mL) served as a positive control. Supernatants were collected after 6 days of culturing, aliquoted, and stored at -80 °C until use (21). IL-21 and IFN-γ produced in the supernatant by stimulated or unstimulated PBMCs were quantified using Luminex kits (ProcartaPlex, Affymetrix eBioscience, Thermo Fisher Scientific, San Diego, CA) according to the manufacturer's instructions. All samples were acquired on a Bioplex-200 instrument (Bio-Rad, Marnes-la-Coquette, France).

Immunophenotype analysis

The phenotypes of isolated mucosal B cells were assessed using FACS-staining with the following antibodies: anti-CD3-BV605 (SK7, BD Biosciences, Le Pont de Claix, France), anti-CD19-PECF594 (HIB19, BD Biosciences), anti-CD10-PECy7 (HI10a, Biolegend, Ozyme, Saint-Quentin en Yveline, France), anti-CD21-BV711 (B-Ly4, BD Biosciences), anti-CD27-APC (L128, BD Biosciences), anti-CD38-PerCP-Cy5.5 (HIT2, Biolegend, Ozyme), anti-IgG-BV421 (G18-145, BD Biosciences), and anti-IgA-FITC (IS11-8E10,

Miltenyi Biotec, Paris, France). Mucosal T_{FH} cells were stained with antibodies to CD3-BV605 (SK7, BD Biosciences), CD4-PECF594 (RP4-T4, BD Biosciences), CXCR5-Alexa 488 (RF8B2, BD Biosciences), and PD1-BV421 (EH12.EH7, Biolegend, Ozyme). For intracellular staining, cells were fixed and permeabilized using the FoxP3 staining buffer set (eBioscience, Thermo Fisher Scientific), washed, and incubated with anti-BCL6-PE (K112-91, BD Biosciences). For all cell stainings, dead cells were excluded from the gating by using the LIVE/DEAD fixable dead-cell stain kit (Molecular Probes, Invitrogen, Saint-Aubin, France). Cytometry acquisition was performed on an LSR II cytometer (BD Biosciences), and the data were analyzed using Flowjo software (Version 7.6.5; TreeStar, Ashland, OR).

B-cell clonality analyses

DNA was extracted from frozen biopsies using the Qiasymphony automated extraction device (Qiagen, Hilden, Germany) according to the manufacturer's instructions. The B-cell repertoire was evaluated by detection of heavy-chain immunoglobulin (IgH) gene rearrangements according to BIOMED-2 guidelines (22). Briefly, three sets of VH primers corresponding to the three VH FR regions (FR1, FR2, and FR3) were used. Each set of primers consisted of six or seven oligonucleotides capable of annealing to their corresponding VH segments (VH1–VH7). These VH primer sets were used in conjunction with a single HEX-labeled JH consensus primer. After PCR, CDR3-derived products were loaded on a 3130 Genetic Analyzer (Applied Biosystems, Foster City, CA) and fragment sizes were analyzed by GeneScan (Thermo Fisher Scientific).

In vitro B-cell differentiation into antibody-secreting cells (ASCs)

Total cell-suspension isolated from rectal biopsies was incubated for 6 days in complete RPMI medium (Gibco) supplemented with 10% FCS, in 96-well plates (Nunc Maxisorp,

Roskilde, Denmark), alone or with immobilized LEAF purified agonist anti-CD40 antibody (5 µg/mL, Biolegend, Ozyme), recombinant human IL-4 (50 ng/ml, Cell Signaling, Ozyme), and IL-21 (50 ng/ml, Cell Signaling, Ozyme). Supernatants from 6-day-old cultures were collected and stored at -20°C.

ELISAs

Polystyrene 96-well ELISA plates (Nunc Maxisorp) were coated with anti-human IgG (2.5 µg/mL, Jackson Immunoresearch, Interchim, Montluçon, France) and anti-human IgA (5 µg/mL, HB200, (23)) in PBS overnight at 4°C. Plates were blocked by 2 hours' incubation with PBS containing 1% BSA (Sigma Aldrich). After washings, the plates were incubated for 2 h with supernatants from cultures of differentiated B cells and 3-fold serial dilutions in PBS-1% BSA. The plates were then washed and incubated for 1 h with HRP-conjugated anti-human IgG, IgA, and IgM antibodies (Jackson Immunoresearch, Interchim). Purified 10-1074 monoclonal IgG (24) and IgA1 (23) antibodies (12 $\mu g \cdot ml^{-1}$ starting concentration) were used as standards. To test HIV-1 gp140 reactivity, purified recombinant YU-2 gp140 trimers were coated (5 µg/mL) on polystyrene 96-well ELISA plates (Nunc Maxisorp) overnight at 4°C in PBS. The plates were then blocked as described above and incubated for 2 h with IgGs secreted in B-cell culture supernatants, adjusted to a concentration of 2 µg/mL in PBS-1% BSA. After washings, the plates were incubated for 1 h with HRP-conjugated anti-human IgG antibodies (Jackson Immunoresearch, Interchim) then revealed using tetramethylbenzidine substrate (TMB, Life Technologies). Anti-HIV-1 gp140 monoclonal IgG antibodies 2F5 and 2G12 (NIH AIDS Reagent Program) were used as positive controls.

Immunohistochemistry

Deparaffinized tissue sections were stained with mouse anti-human Pax-5 (DAK-*Pax5*, Dako Cytomation, Glostrup, Denmark) and rabbit anti-human PD-L1 (E1L3N, Cell Signaling, Ozyme) antibodies then with the anti-rabbit and anti-mouse IgG avidin–biotin complex system (ABC kit universal, Vectastain, Vector Laboratories, Les Ulis, France). Cell staining was performed using the DAB Substrate Kit for peroxidase (Vector Laboratories). All slides were counterstained with hematoxylin. Immunohistochemical images were acquired on a Zeiss Axioplan 2 (Göttingen, Germany) microscope equipped with an X20 (0.45 NA) objective, using a Zeiss Mrc digital camera (Göttingen, Germany) and AxioVision microscope software (Zeiss).

Real-time quantitative PCR analysis

Total RNAs were isolated from rectal biopsies using the RNeasy Micro Kit (Qiagen) according to the manufacturer's protocol then retrotranscribed into cDNA molecules using the Affinity Script QPCR cDNA synthesis kit (Agilent, Santa Clara, CA). Quantitative PCRs were performed using the Brilliant II SYBR GREEN Q-PCR kit (Agilent) on the Mx3005 QPCR Machine (Agilent). OAZ-1 mRNA, whose expression was found to be stable across the three groups of participants, was used as a control for sample normalization. The relative levels of each gene were calculated using the $2^{-\Delta\Delta CT}$ method.

The following primers were used (forward/reverse, 5'- 3'):

OAZ-1, ACTTATTCTACTCCGATGATCGAGAATCCTCGTCTTGTC (Invitrogen);

IL-6, CTCAGCCCTGAGAAAGGAGATTCTGCCAGTGCCTCTTTGC (Eurofins Genomics, Les Ulis, France);

IL-27p28 Ref Seq Accession no. NM_145659.3 (Qiagen);

EBI-3, Ref Seq Accession no. NM_005755.2 (Qiagen);

AICDA, Ref Seq Accession no. NM_020661 (Qiagen);

IL-12A, AATGTTCCCATGCCTTCACCCAATCTCTTCAGAAGTGCAAGGG (Eurofins Genomics).

Statistics

Groups were compared using either the two-sided Mann-Whitney U test or the Kruskal-Wallis test. Spearman's rank test was applied to assess bivariate correlations and linear regression analysis performed to produce an accompanying best-fit line. All statistical analyses were performed using GraphPad Prism (version 6.0, GraphPad Software, La Jolla, CA).

RESULTS

Early treatment preserved mucosal resting memory B cells

The phenotypes of cells freshly isolated from rectal biopsies were compared in HIV-1-infected patients given e-ART (n=7) or l-ART (n=8) and in HIV-negative controls (n=6). Table 1 reports the characteristics of the participants. Absolute counts of total $CD19^+$ B cells were significantly higher in the l-ART groups than in the control groups, with no difference between the e-ART and l-ART groups (**Figure 1a**). No differences were observed in term of $CD19^+$ B cells frequency between HIV1-infected groups and controls. By assessing differences in surface CD27 and CD21 expression in $CD19^+$ $CD38^{low}$ $CD10^-$ B cells, we identified mature naive (MN, $CD27^-$ $CD21^+$), resting memory (RM, $CD27^+$ $CD21^+$), tissue-like memory (TLM, $CD27^-$ $CD21^-$), and activated memory (AM, $CD27^+$ $CD21^-$) B cells (**Figure 1b**). As shown in **Figure 1c**, patients in both the cART groups exhibited lower frequencies of AM B cells (1.3%±0.5% and 1.6%±0.4%, respectively) compared to the controls (4.4%±1.5%) (P<0.001 for both comparisons). Other B-cell subsets in e-ART patients were comparable to those from controls but differed significantly from those in l-ART patients, who had a lower frequency of RM B cells (39.6%±10.8% *vs.* 71.8%±15%, P<0.001) and higher frequencies of MN and TLM B cells (54.5%±11.6% and 2.6%±0.9% *vs.* 23.3%±14.1% and 0.9%±0.6%, P<0.001 and P<0.01, respectively). Blood B-cell phenotype was not substantially different between the e-ART and l-ART groups (**Supplemental Figure 1**).

Mucosal antibody-secreting cells from late-treated patients displayed an immunoglo-bulin profile skewed towards IgGs

The frequencies of terminally differentiated B cells (antibody-secreting cells [ASCs], defined as $CD19^+$ $CD27^{hi}$ $CD38^+$ $CD10^-$), known to be abundant in the gut mucosa (25), were

comparable in the e-ART and l-ART groups (38.5%±15.9% *vs.* 30.7%±13.3%, respectively) (**Figure 2a**) but were significantly lower than in the control group (71.7%±12.3%, $P<0.001$ for both comparisons). The total amount of immunoglobulins spontaneously released by freshly isolated mucosal ASCs cultured for 6 days was not different between the e-ART and l-ART groups (data not shown). In contrast, significant differences were noted regarding the immunoglobulin isotype profile. Thus, IgA release by ASCs from e-ART patients was greater compared to ASCs from l-ART patients (9.4±13.4 µg/mL *vs.* 2.8±1.4 µg/mL, $P<0.05$, respectively) and similar to that seen with ASCs from controls (**Figure 2b**). In contrast, the total amount of IgGs released by ASCs was significantly greater in the l-ART group than in the e-ART group (6.4±5.8 µg/mL *vs.* 2.5±1.5 µg/mL, $P<0.05$) (**Figure 2b**). The IgA/IgG ratio indicated skewing from IgAs to IgGs in the l-ART group compared to the e-ART group (0.68±0.72 AU *vs.* 9.4±15.24 AU, $P<0.001$) (data not shown). The IgA/IgG ratio differed significantly between the l-ART and control groups (0.68±0.72 AU *vs.* 2.89±1.93 AU, $P<0.05$) but was comparable between the e-ART and control groups (9.4±15.24 AU *vs.* 2.89±1.93 AU, $P=0.289$).

To evaluate whether the time of cART initiation might influence the mucosal B-cell repertoire in HIV-1-infected individuals, we studied B-cell clonality in the e-ART and l-ART groups (26). All patients in both groups displayed a normally distributed, polyclonal profile (**Figure 2c**) similar to that typically observed in healthy humans (27). Interestingly, some of the treated patients exhibited abnormal, preeminent, single peaks in their immunoglobulin spectratype (**Figure 2d**), suggesting clonal B-cell expansions in ectopic mucosal lymphoid structures such as those described in reactive lymphoproliferation (28, 29). Interestingly, these peaks were more common in the e-ART group than in the l-ART group, although the difference was not statistically significant (25% *vs.* 8.3%, $P=0.34$) (**Figure 2e**).

CD4$^+$ T follicular helper (T_{FH}) cells are expanded in the mucosa of early-treated HIV-1-infected patients

The development of memory B cells within GC follicles depends heavily on the presence of T_{FH} cells (30). The frequency of mucosal T_{FH} cells, defined as $CD3^+CD4^+PD1^{hi}CXCR5^+Bcl6^+$ cells (**Figure 3a**), was significantly higher in the e-ART group than in the l-ART group (9.5%±5.1% *vs.* 1.6%±1.5% of $CD3^+$ $CD4^+$ cells, $P<0.05$); the values in the e-ART and l-ART groups were significantly higher than in the controls (0.3%±0.3%, $P<0.0001$ and $P<0.05$, respectively) (**Figure 3b**). As shown in **Figure 3c**, the frequency of T_{FH} cells correlated significantly with the frequency of RM B cells (r=0.7542, $P<0.01$). As illustrated in **Figure 3d**, an analysis of differential CXCR3 and CCR6 expression (31) allowed us to define three main circulating-T_{FH} (c-T_{FH}) cell subsets within blood $CCR7^-$ $CXCR5^+CD4^+$T cells: $CXCR3^+CCR6^-$ (c-T_{FH}1), $CXCR3^-CCR6^-$ (c-T_{FH}2), and $CXCR3^-CCR6^+$ (c-T_{FH}17). No differences in frequency or phenotype of c-T_{FH} cells were observed between the e-ART and l-ART patients (**Figure 3e**).

Interaction between T_{FH} cells and B cells in the gut of early-treated patients may promote antibody generation

The above-reported results and the role for PD-$L1^{hi}$ B cells in regulating T_{FH}-cell expansion and function (8, 10) led us to investigate whether PD-L1 expression in mucosal follicles differed between the e-ART and l-ART groups. Single-cell expression of Pax5 and PD-L1 was sought by immunohistochemistry of rectal biopsies from e-ART (n=6) and l-ART (n=6) patients (**Figure 4a**). Based on Pax5 staining, B-cell follicle architecture differed between the two groups. All e-ART patients displayed well-defined secondary follicles, whereas most l-ART patients had some degree of B lymphoid area disorganization, with diffuse B-cell distribution in four of the six biopsies (patients g, h, j and m). PD-L1 expression

was clearly detectable in a single e-ART patient (patient e) and was not located in the B-cell area (**Figure 4a**). In contrast, PD-L1 expression was high in the follicles of five of the six biopsies from l-ART patients and was located within the B-cell area in three of these five biopsies (patients g, k, h) (**Figure 4b**).

Previous studies have established the importance of soluble factors such as IL-6 and IL-27 for the development and maintenance of T_{FH} cells in mice and humans (32, 33). We used real-time quantitative polymerase chain reaction technology (RT-qPCR) to quantify the transcripts for IL-6 and the two IL-27 subunits (IL-27p28 and EBI3) in the rectal biopsies from patients in both HIV-1-positive groups (**Supplemental figure 2**). All three mRNAs were expressed at significantly higher levels in the e-ART group than the l-ART group (IL-6 mRNA: 4.39±6.14 AU *vs.* 0.76±0.57 AU, $P<0.05$; IL-27p28 mRNA: 0.12±0.22 AU *vs.* 0.04±0.03 AU, $P<0.05$; and EBI3 mRNA: 0.21±0.09 AU *vs.* 0.08±0.04 AU, $P<0.05$). The expression of control mRNAs encoding the IL-12A subunit, which also dimerize with EBI3 to form IL-35, was not different between the two HIV-positive groups (0.51±0.06 AU *vs.* 0.49±0.15 AU; $P=0.4127$). Crosstalk between B cells and T_{FH} cells was investigated by RT-qPCR quantification of activation-induced cytidine deaminase (AID) transcripts. AID mRNA expression tended to be higher in mucosal GCs from e-ART patients compared to l-ART patients without reaching significance (**Supplemental Figure 2,** 0.07±0.11 AU *vs.* 0.006±0.007 AU, $P=0.111$).

Mucosal HIV-1 envelope-reactive memory B cells were expanded in early-treated HIV-1-infected patients

Next, we investigated whether HIV-1-specific B-cell responses were affected by the timing of cART initiation. We used flow cytometry to evaluate the frequency and phenotype of YU-2 gp140-reactive B cells. **Figure 5a** shows representative dot plots of $CD19^+$ gp140-

reactive cells from the patients and controls. Importantly, the frequency of mucosal gp140-reactive $CD19^+$ cells was significantly higher in the e-ART group than in the l-ART group (0.26%±0.09% *vs.* 0.07%±0.05%, $P<0.01$) (**Figure 5b**) and the phenotype of these cells differed between the two groups **(Figure 5c)**, with a predominance of RM cells in the e-ART group and a mixture of MN and RM cells in the l-ART group. Moreover, the frequency of mucosal gp140-reactive RM B cells was significantly higher in the e-ART group compared to the l-ART group (0.22%±0.14% *vs.* 0.05%±0.08%, $P<0.05$) (**Figure 5c**). In line with these results, the frequency of gp140-reactive B cells expressing membrane-bound IgG was significantly higher in the e-ART group than in the l-ART group (0.28%±0.18% *vs.* 0.06%±0.04%, $P<0.05$) (**Figure 5d**). Finally, the frequency of total mucosal gp140-reactive B cells correlated significantly with that of T_{FH} cells in the HIV-infected patients (r=0.7821, $P<0.001$) (**Figure 5e**). We used an ELISA against trimeric YU-2 gp140 to test supernatants of freshly isolated mucosal B cells from both groups of HIV-1-infected patients, after 6 days of stimulation. In the e-ART group, compared to unstimulated mucosal B cells, stimulated cells released larger amounts of gp140-reactive IgGs (0 AU *vs.* 0.21±0.27 AU, $P<0.01$) (**Figure 5f**). Stimulation did not have this effect on cells from the l-ART group (**Figure 5f**).

PBMCs from early-treated patients released larger amounts of IL-21 in response to stimulation with pools of HIV-1 peptides

To further investigate the association between the time of cART initiation and the role for T_{FH} cells in the development of HIV-1-specific B-cell responses, we evaluated IL-21 production by PBMC. Indeed, IL-21 is primarily produced by $CD4^+$ T cells and is particularly critical to generation of antigen-specific IgG antibodies and expansion of class-switched B cells and plasma cells *in vivo.* Blood IL-21 secreting $CD4^+$ T cells share phenotypic and transcriptional similarities with lymphoid T_{FH} cells in HIV-1-infected individuals (34). Given

the very limited number of total cells that can be retrieved from rectal biopsies, we used blood samples to quantify HIV-1-specific IL-21^{+} and HIV-1-specific IFN-γ^{+} T cells in both HIV-1-positive groups. PBMCs stimulated with staphylococcal enterotoxin B (SEB) released significantly more IL-21 in the e-ART group than in the l-ART group (43.9±35.9 pg/mL *vs.* 10.9±9.4 pg/mL $P<0.01$) (**Figure 6a, left panel**). Similarly, SEB-stimulated PBMCs released more IFN-γ in the e-ART group than in the l-ART group (17 866.5±9 512.6 pg/mL *vs.* 9 186.4±11 244.4 pg/mL, $P<0.05$) (**Figure 6a, right panel**). In addition, IL-21 release by PBMCs stimulated with pools of HIV-1 Env and Gag peptides was significantly more marked in the e-ART group (5.3±3.5 pg/mL *vs.* 2.7±2.9 pg/mL in the l-ART group, $P<0.05$) (**Figure 6b**). In contrast, no statistically significant differences were observed between the e-ART and l-ART groups for the secretion of IFN-γ by PBMCs stimulated with HIV-1 Env and Gag peptides (**Figure 6b**). In line with these results, the frequency of gp140-reactive B cells in blood was higher in the e-ART group (0.21%±0.12% *vs.* 0.1%±0.07%, $P<0.05$) (**Supplemental Figure 3**)

DISCUSSION

Previous studies have shown that persistent infection with viruses such as the HIV-1 lead to severe abnormalities in the dynamics of B-cell distribution and function in the blood and lymphoid organs, which very likely interfere with the establishment of an optimal antiviral humoral response (35). Far less is known about whether these alterations also occur in the gut mucosa and whether the timing of cART initiation influences B-cell phenotype and function. Our previous gene profiling study distinguished two groups of patients, based on pathway signatures of gut mucosal lymphoid structures and dendritic-cell function, which perfectly matched the timing of cART initiation (17). Here, we extend those data by demonstrating, at the cellular level, that early cART initiation preserves gut TLSs, which may function as active ectopic GCs characterized by high frequencies of functional T_{FH} and gp140-reactive memory B cells. These GCs may play a critical role in the development of the antibody response.

In the gut, e-ART was associated with partial correction of the abnormal expansion of activated memory and TLM B cells and with preservation of RM B cells, conferring on e-ART patients a phenotype comparable to that of uninfected controls. In contrast, patients treated only at the chronic stage, despite experiencing long-term control of HIV replication, exhibited a profile suggesting impaired B-cell maturation, with a significant reduction in RM B cells. Finally, both groups of HIV-1-infected patients had similarly lower frequencies of ASCs compared to the uninfected control group. In contrast to findings at the mucosal levels, we did not find significant differences in the blood of early and late treated patients. These results differ from results reported by others (15, 36), and might be explained by a longer duration of ART treatment (more than 10 years on with an average of 4-21 years) in our cohort of l-ART patients. On the other hand, according to our results, a partial restoration of a normal homeostasis of B-cell populations with a decrease of activated memory and tissue-like

memory B cells has been reported in chronically ART treated patients (37, 38). Altogether, our results underscore the interest to study changes in B cell populations in various compartments revealing here that if e-ART may limit the major B-cell subset alterations in the gut, they are only partially restored even in the long term.

Although ASC frequencies in the gut were comparable in the e-ART and l-ART groups, the proportion of IgG-secreting cells was higher and the proportion of IgA-secreting cells commensurately lower in the l-ART group. The abnormal predominance of IgG in l-ART patients may reflect mucosal inflammation, which may contribute to impair gut mucosal homeostasis, as observed in inflammatory bowel disease (39). Moreover, the IgA secretion deficiency may cause changes in the composition of the intestinal microbiota (40) that may further activate the inflammatory processes seen in the gut of patients with chronic HIV-1 infection despite effective cART (41). The skewing of IgA-secreting cells toward IgG-secreting cells is probably linked to microbial translocation and noninfectious complications associated with systemic inflammation. We therefore looked for abnormalities in global mucosal B-cell repertoires in the e-ART and l-ART groups, using the spectratyping method. Surprisingly, all HIV-1 infected patients displayed polyclonal profiles, although single expansions were noted, more often in the e-ART group than in the l-ART group. However, the global repertoire analyses by immunoglobulin spectratyping were performed on mucosal immunoglobulin-expressing and -secreting cells in the gut, including a high proportion of ASCs resulting from T-cell-independent differentiation of mucosal B cells. Given the massive T-cell depletion associated with HIV-1 infection (42), complete disorganization of ectopic mucosal GCs (17, 43), and crucial role for these GCs in memory B-cell development within TLSs (44), any disturbances in the B-cell repertoire would mainly concern the GC B cells (6) rather than the T-cell-independent ASCs.

In GCs, T_{FH} cells are strongly involved in the development of memory B cells. Here, we found that T_{FH} cells were expanded in the gut of HIV-1-infected patients compared to controls. Importantly, the frequency of gut T_{FH} cells correlated with the frequency of RM B cells in the gut. These results are in line with previous reports showing T_{FH} cell expansion in lymph node, spleen, and gut tissues of rhesus macaques infected with the SIV (45, 46) and in mucosal tissues from humanized-DRAG mouse models of HIV-1 infection (47). T_{FH} cells decreased substantially with cART (6). Surprisingly, gut T_{FH} remained significantly higher in the e-ART group than in the l-ART group whereas no differences were observed for cT_{FH} frequency between the two groups. Our results underline the critical impact of tissue compartmentalization on T_{FH} cell and B cells dynamics during HIV infection. In SIV infected rhesus macaques (RMs), T_{FH} dynamics differs from one compartment to another (peripheral blood, vs LNs or spleen) (48). Indeed, microenvironment is essential for the differentiation and the maintenance of T_{FH} cells. In the gut, the microbiota induces the differentiation of $CD4^+$ T cells into T_{FH} cells, thereby promoting the secretion of microbial-specific IgAs, which are important for controlling the microflora and maintaining gut homeostasis (49). Thus, T_{FH} expansion in HIV-1-infected patients may be seen as a mechanism that compensates for the massive Th17 depletion, thereby helping to maintain gut homeostasis. This hypothesis is supported by studies in RORγt-deficient mice, in which large numbers of TLSs are required to contain the microbiota (50).

453 T_{FH} dynamics varies according to the severity of the disease. Slow progressor RMs display an
454 increased frequency of T_{FH} cells in LNs whereas their numbers drastically decreased in fast
455 progressors RMs (51, 52). Evidences support the pivotal role of persistent viral antigen within
456 the GC in driving T_{FH} cell expansion and the disruption of GC organization coincides with the
457 loss of T_{FH} cells and the onset of AIDS in terminal stages of HIV infection (51). CXCL13 has
458 been described to be a plasma biomarker of germinal center activity in HIV-infected humans
459 (53). In our cohort of 56 l-ART patients and 17 e-ART patients, CXCL13 tended to be higher
460 in the sera of e-ART patients compared to l-ART patients without reaching significance (data
461 not shown). We have previously reported a loss of FDC network and TLS in the gut of l-ART
462 patients. Thus, this may impact T_{FH} maintenance in l-ART patients.
463 The difference of T_{FH} frequencies between e-ART and l-ART patients may also reflect
464 distinct immune response of T_{FH} cells depending on the nature of help signals, consisting of
465 both cytokines and cell surface molecules. We therefore investigated the signaling factors that
466 contribute to T_{FH} expansion. Studies in SIV-infection models (46) and in mice (33)
467 established a key role for IL-6 and IL-27 signaling in T_{FH} cell function and GC responses. In
468 our study, IL-6 and IL-27 transcript levels in the gut were higher wit e-ART than with l-ART.
469 In addition to signaling mediators, B-cell dysregulation may also be involved in the reduced
470 frequency and impaired function of T_{FH} cells in HIV-1 infection (8). PD-L1 expression on B
471 cells and PD-1 receptor engagement on T_{FH} cells decrease IL-21 secretion and cell
472 proliferation (8, 10). We found that the proportion of TLS B cells expressing PD-L1 was
473 greater in the l-ART group than in the e-ART group. These results suggest that e-ART
474 patients had functional T_{FH} cells capable of contributing to the development of antigen-
475 specific B-cell responses in gut GCs.
476

Recent work highlighted the importance of maintaining functional GCs for the development of HIV-1 bNAbs (54). We therefore hypothesized that functional HIV-1-specific T_{FH} cells enhanced HIV-1-specific B-cell responses in the gut. In keeping with this hypothesis, the frequencies of T_{FH} and gp140-reactive memory B cells in gut TLSs were higher in the e-ART group than in the l-ART group. Interestingly, the frequency of gut T_{FH} cells correlated with the frequency of gut gp140-reactive memory B cells in cART-treated HIV-1-infected patients. In line with these results, it has been recently shown that HIV Env-specific $CXCR5^+$ $CD4^+$ T cells that secrete interleukin-21 are strongly associated with B cell memory phenotypes and function (55). The results suggested that circulating total and HIV-1-specific IL-21-producing T cells were more abundant with e-ART than with l-ART. In contrast, counts of circulating IFN-γ-secreting HIV-1-specific T cells were not significantly different between the two groups. It is tempting to speculate that the HIV-1 specificity of gut T_{FH} cells may be extrapolated from the amount of IL-21 released by T cells in response to stimulation with a pool of HIV-1 peptides. Thus, TLSs may act as active ectopic GCs and may play a critical role in the development of the affinity-matured HIV-1-specific antibody response.

The first HIV-1-reactive antibodies become detectable about 13 days after HIV-1 transmission (56) and are mainly directed against the Env gp41, in both blood and the terminal ileum. Most of these gp41 antibodies are polyreactive affinity-matured IgGs that target self- and microbial antigens (57). Using an *in vitro* B-cell-to-ASC differentiation assay, we confirmed that the frequency of gp140-reactive memory B cells was higher with e-ART than with l-ART, as shown by the larger amount of anti-gp140 reactive IgGs detectable by ELISA in the e-ART group. The anti-gp140 IgGs targeted the gp41 portion of the HIV-1 Env protein (data not shown). Mucosal B-cell clones can re-enter a germinal center, where they undergo further somatic hypermutation to produce high-affinity IgA that is adapted to the

changing composition of the microbiota. It is tempting to speculate that gp140-reactive memory B cells may be a good target for therapeutic vaccine. Indeed, a recent study of the pre-vaccination B-cell repertoire identified a preexisting pool of microbiome-gp41 cross-reactive B cells that was stimulated by the vaccine (58). Extensive molecular characterization of the gp-140-reactive B cells would be important to explore the potential beneficial effects of e-ART on the development of a potent HIV-1-specific humoral immune response in the gut.

The beneficial impact of e-ART on the circulating B-cell populations is now well-documented (15). Here, we demonstrated that e-ART may also lessen the alterations in mucosal B-cell subsets. The protection afforded by a potent mucosal humoral response is particularly important in the gut, where the intestinal barrier is continuously attacked by the microbiota. GC preservation may contribute to diversification of the mucosal B-cell repertoire, thereby helping to control the billions of microorganisms found in the gut lumen (59). Thus, e-ART may contribute to reduce the appearance of non-HIV-1 AIDS-related gastrointestinal syndromes. Considerable effort is being put into creating a vaccine-based strategy for developing HIV-1 bNAbs in infected patients. A common feature of bNAbs is a higher level of somatic hypermutations compared to that seen in typical immune responses (60, 61), which is generated after multiple cell passages through GCs containing target antigens. We demonstrated that e-ART helped to preserve intestinal GC functions and was associated with a higher frequency of HIV-1 Env gp140-specific B cells in the gut compared to l-ART. This finding suggests that eliciting potent anti-HIV-1 antibodies at mucosal sites may require e-ART, to maintain an optimal mucosal GC response by preserving T_{FH} cells function and, therefore, maturing GC B cells.

Acknowledgments

The HIV-1 Env gp41 (0671) was obtained from the center for AIDS Reagents, NIBSC, UK supported by EURIPRED (EC FP7 INFRASTRUCTURES-2012-INFRA-2012-1.1.5.: Grant Number 31266). This work was supported by the SIDACTION foundation, the ANRS and the Labex Vaccine Research Institute (VRI) (Investissements d'Avenir program managed by the ANR under reference ANR-10-LABX-77-01).

Author contributions

SH and YL conceived and supervised the study.

SH, YL, HM, and CP designed the experiments and analyzed the data.

CP, CI, MS, CC, MF, and MHDL performed the experiments.

LH, SG, LL, TP, and ML recruited the participants and collected the samples.

SH, YL, HM, and CP wrote the manuscript, with contributions from all authors.

References

1. Tomaras, G. D., and B. F. Haynes. 2009. HIV-1-specific antibody responses during acute and chronic HIV-1 infection. *Current opinion in HIV and AIDS* 4: 373-379.
2. Mouquet, H. 2014. Antibody B cell responses in HIV-1 infection. *Trends in immunology* 35: 549-561.
3. Kelsoe, G., and B. F. Haynes. 2017. Host controls of HIV broadly neutralizing antibody development. *Immunological reviews* 275: 79-88.
4. Crotty, S. 2014. T follicular helper cell differentiation, function, and roles in disease. *Immunity* 41: 529-542.
5. Perreau, M., A. L. Savoye, E. De Crignis, J. M. Corpataux, R. Cubas, E. K. Haddad, L. De Leval, C. Graziosi, and G. Pantaleo. 2013. Follicular helper T cells serve as the major CD4 T cell compartment for HIV-1 infection, replication, and production. *The Journal of experimental medicine* 210: 143-156.
6. Lindqvist, M., J. van Lunzen, D. Z. Soghoian, B. D. Kuhl, S. Ranasinghe, G. Kranias, M. D. Flanders, S. Cutler, N. Yudanin, M. I. Muller, I. Davis, D. Farber, P. Hartjen, F. Haag, G. Alter, J. Schulze zur Wiesch, and H. Streeck. 2012. Expansion of HIV-specific T follicular helper cells in chronic HIV infection. *The Journal of clinical investigation* 122: 3271-3280.
7. Locci, M., C. Havenar-Daughton, E. Landais, J. Wu, M. A. Kroenke, C. L. Arlehamn, L. F. Su, R. Cubas, M. M. Davis, A. Sette, E. K. Haddad, A. V. I. P. C. P. I. International, P. Poignard, and S. Crotty. 2013. Human circulating PD-1+CXCR3-CXCR5+ memory Tfh cells are highly functional and correlate with broadly neutralizing HIV antibody responses. *Immunity* 39: 758-769.
8. Cubas, R. A., J. C. Mudd, A. L. Savoye, M. Perreau, J. van Grevenynghe, T. Metcalf, E. Connick, A. Meditz, G. J. Freeman, G. Abesada-Terk, Jr., J. M. Jacobson, A. D. Brooks, S. Crotty, J. D. Estes, G. Pantaleo, M. M. Lederman, and E. K. Haddad. 2013. Inadequate T follicular cell help impairs B cell immunity during HIV infection. *Nature medicine* 19: 494-499.
9. Finnefrock, A. C., A. Tang, F. Li, D. C. Freed, M. Feng, K. S. Cox, K. J. Sykes, J. P. Guare, M. D. Miller, D. B. Olsen, D. J. Hazuda, J. W. Shiver, D. R. Casimiro, and T. M. Fu. 2009. PD-1 blockade in rhesus macaques: impact on chronic infection and prophylactic vaccination. *J Immunol* 182: 980-987.
10. Khan, A. R., E. Hams, A. Floudas, T. Sparwasser, C. T. Weaver, and P. G. Fallon. 2015. PD-L1hi B cells are critical regulators of humoral immunity. *Nature communications* 6: 5997.
11. Planes, R., L. BenMohamed, K. Leghmari, P. Delobel, J. Izopet, and E. Bahraoui. 2014. HIV-1 Tat protein induces PD-L1 (B7-H1) expression on dendritic cells through tumor necrosis factor alpha- and toll-like receptor 4-mediated mechanisms. *J Virol* 88: 6672-6689.
12. Moir, S., and S. F. Anthony. 2013. Insights into B cells and HIV-specific B-cell responses in HIV-infected individuals. *Immunological Reviews* 254.
13. Moir, S., J. Ho, A. Malaspina, W. Wang, A. C. DiPoto, M. A. O'Shea, G. Roby, S. Kottilil, J. Arthos, M. A. Proschan, T. W. Chun, and A. S. Fauci. 2008. Evidence for HIV-associated B cell exhaustion in a dysfunctional memory B cell compartment in HIV-infected viremic individuals. *The Journal of experimental medicine* 205: 1797-1805.
14. Pensieroso, S., L. Galli, S. Nozza, N. Ruffin, A. Castagna, G. Tambussi, B. Hejdeman, D. Misciagna, A. Riva, M. Malnati, F. Chiodi, and G. Scarlatti. 2013. B-cell subset alterations and correlated factors in HIV-1 infection. *Aids* 27: 1209-1217.
15. Moir, S., C. M. Buckner, J. Ho, W. Wang, J. Chen, A. J. Waldner, J. G. Posada, L. Kardava, M. A. O'Shea, S. Kottilil, T. W. Chun, M. A. Proschan, and A. S. Fauci. 2010. B cells in early and chronic HIV infection: evidence for preservation of immune function associated with early initiation of antiretroviral therapy. *Blood* 116: 5571-5579.
16. Cagigi, A., A. Nilsson, S. Pensieroso, and F. Chiodi. 2010. Dysfunctional B-cell responses during HIV-1 infection: implication for influenza vaccination and highly active antiretroviral therapy. *The Lancet. Infectious diseases* 10: 499-503.

17. Kok, A., L. Hocqueloux, H. Hocini, M. Carriere, L. Lefrou, A. Guguin, P. Tisserand, H. Bonnabau, V. Avettand-Fenoel, T. Prazuck, S. Katsahian, P. Gaulard, R. Thiebaut, Y. Levy, and S. Hue. 2015. Early initiation of combined antiretroviral therapy preserves immune function in the gut of HIV-infected patients. *Mucosal immunology* 8: 127-140.
18. Fiebig, E. W., D. J. Wright, B. D. Rawal, P. E. Garrett, R. T. Schumacher, L. Peddada, C. Heldebrant, R. Smith, A. Conrad, S. H. Kleinman, and M. P. Busch. 2003. Dynamics of HIV viremia and antibody seroconversion in plasma donors: implications for diagnosis and staging of primary HIV infection. *AIDS* 17: 1871-1879.
19. Mouquet, H., F. Klein, J. F. Scheid, M. Warncke, J. Pietzsch, T. Y. Oliveira, K. Velinzon, M. S. Seaman, and M. C. Nussenzweig. 2011. Memory B cell antibodies to HIV-1 gp140 cloned from individuals infected with clade A and B viruses. *PloS one* 6: e24078.
20. Mouquet, H., L. Scharf, Z. Euler, Y. Liu, C. Eden, J. F. Scheid, A. Halper-Stromberg, P. N. Gnanapragasam, D. I. Spencer, M. S. Seaman, H. Schuitemaker, T. Feizi, M. C. Nussenzweig, and P. J. Bjorkman. 2012. Complex-type N-glycan recognition by potent broadly neutralizing HIV antibodies. *Proceedings of the National Academy of Sciences of the United States of America* 109: E3268-3277.
21. Surenaud, M., C. Manier, L. Richert, R. Thiebaut, Y. Levy, S. Hue, and C. Lacabaratz. 2016. Optimization and evaluation of Luminex performance with supernatants of antigen-stimulated peripheral blood mononuclear cells. *BMC immunology* 17: 44.
22. McDonald, T. J., L. Kuo, and F. C. Kuo. 2017. Determination of VH Family Usage in B-Cell Malignancies via the BIOMED-2 IGH PCR Clonality Assay. *American journal of clinical pathology* 147: 549-556.
23. Lorin, V., and H. Mouquet. 2015. Efficient generation of human IgA monoclonal antibodies. *Journal of immunological methods* 422: 102-110.
24. Malbec, M., F. Porrot, R. Rua, J. Horwitz, F. Klein, A. Halper-Stromberg, J. F. Scheid, C. Eden, H. Mouquet, M. C. Nussenzweig, and O. Schwartz. 2013. Broadly neutralizing antibodies that inhibit HIV-1 cell to cell transmission. *The Journal of experimental medicine* 210: 2813-2821.
25. Landsverk, O. J., O. Snir, R. B. Casado, L. Richter, J. E. Mold, P. Reu, R. Horneland, V. Paulsen, S. Yaqub, E. M. Aandahl, O. M. Oyen, H. S. Thorarensen, M. Salehpour, G. Possnert, J. Frisen, L. M. Sollid, E. S. Baekkevold, and F. L. Jahnsen. 2017. Antibody-secreting plasma cells persist for decades in human intestine. *The Journal of experimental medicine* 214: 309-317.
26. Guzman, L. M., D. Castillo, and S. O. Aguilera. 2010. Polymerase chain reaction (PCR) detection of B cell clonality in Sjogren's syndrome patients: a diagnostic tool of clonal expansion. *Clinical and experimental immunology* 161: 57-64.
27. Dong, L., Y. Masaki, T. Takegami, Z. X. Jin, C. R. Huang, T. Fukushima, T. Sawaki, T. Kawanami, T. Saeki, K. Kitagawa, S. Sugai, T. Okazaki, Y. Hirose, and H. Umehara. 2007. Clonality analysis of lymphoproliferative disorders in patients with Sjogren's syndrome. *Clinical and experimental immunology* 150: 279-284.
28. Langerak, A. W., T. J. Molina, F. L. Lavender, D. Pearson, T. Flohr, C. Sambade, E. Schuuring, T. Al Saati, J. J. van Dongen, and J. H. van Krieken. 2007. Polymerase chain reaction-based clonality testing in tissue samples with reactive lymphoproliferations: usefulness and pitfalls. A report of the BIOMED-2 Concerted Action BMH4-CT98-3936. *Leukemia* 21: 222-229.
29. Evans, P. A., C. Pott, P. J. Groenen, G. Salles, F. Davi, F. Berger, J. F. Garcia, J. H. van Krieken, S. Pals, P. Kluin, E. Schuuring, M. Spaargaren, E. Boone, D. Gonzalez, B. Martinez, R. Villuendas, P. Gameiro, T. C. Diss, K. Mills, G. J. Morgan, G. I. Carter, B. J. Milner, D. Pearson, M. Hummel, W. Jung, M. Ott, D. Canioni, K. Beldjord, C. Bastard, M. H. Delfau-Larue, J. J. van Dongen, T. J. Molina, and J. Cabecadas. 2007. Significantly improved PCR-based clonality testing in B-cell malignancies by use of multiple immunoglobulin gene targets. Report of the BIOMED-2 Concerted Action BHM4-CT98-3936. *Leukemia* 21: 207-214.
30. Rankin, A. L., H. MacLeod, S. Keegan, T. Andreyeva, L. Lowe, L. Bloom, M. Collins, C. Nickerson-Nutter, D. Young, and H. Guay. 2011. IL-21 receptor is critical for the development of memory B cell responses. *Journal of immunology* 186: 667-674.

31. Morita, R., N. Schmitt, S. E. Bentebibel, R. Ranganathan, L. Bourdery, G. Zurawski, E. Foucat, M. Dullaers, S. Oh, N. Sabzghabaei, E. M. Lavecchio, M. Punaro, V. Pascual, J. Banchereau, and H. Ueno. 2011. Human blood CXCR5(+)CD4(+) T cells are counterparts of T follicular cells and contain specific subsets that differentially support antibody secretion. *Immunity* 34: 108-121.
32. Nurieva, R. I., Y. Chung, D. Hwang, X. O. Yang, H. S. Kang, L. Ma, Y. H. Wang, S. S. Watowich, A. M. Jetten, Q. Tian, and C. Dong. 2008. Generation of T follicular helper cells is mediated by interleukin-21 but independent of T helper 1, 2, or 17 cell lineages. *Immunity* 29: 138-149.
33. Batten, M., N. Ramamoorthi, N. M. Kljavin, C. S. Ma, J. H. Cox, H. S. Dengler, D. M. Danilenko, P. Caplazi, M. Wong, D. A. Fulcher, M. C. Cook, C. King, S. G. Tangye, F. J. de Sauvage, and N. Ghilardi. 2010. IL-27 supports germinal center function by enhancing IL-21 production and the function of T follicular helper cells. *The Journal of experimental medicine* 207: 2895-2906.
34. Schultz, B. T., J. E. Teigler, F. Pissani, A. F. Oster, G. Kranias, G. Alter, M. Marovich, M. A. Eller, U. Dittmer, M. L. Robb, J. H. Kim, N. L. Michael, D. Bolton, and H. Streeck. 2016. Circulating HIV-Specific Interleukin-21(+)CD4(+) T Cells Represent Peripheral Tfh Cells with Antigen-Dependent Helper Functions. *Immunity* 44: 167-178.
35. Moir, S., and A. S. Fauci. 2009. B cells in HIV infection and disease. *Nature reviews. Immunology* 9: 235-245.
36. van Grevenynghe, J., R. A. Cubas, A. Noto, S. DaFonseca, Z. He, Y. Peretz, A. Filali-Mouhim, F. P. Dupuy, F. A. Procopio, N. Chomont, R. S. Balderas, E. A. Said, M. R. Boulassel, C. L. Tremblay, J. P. Routy, R. P. Sekaly, and E. K. Haddad. 2011. Loss of memory B cells during chronic HIV infection is driven by Foxo3a- and TRAIL-mediated apoptosis. *The Journal of clinical investigation* 121: 3877-3888.
37. Luo, Z., L. Ma, L. Zhang, L. Martin, Z. Wan, S. Warth, A. Kilby, Y. Gao, P. Bhargava, Z. Li, H. Wu, E. G. Meissner, Z. Li, J. M. Kilby, G. Liao, and W. Jiang. 2016. Key differences in B cell activation patterns and immune correlates among treated HIV-infected patients versus healthy controls following influenza vaccination. *Vaccine* 34: 1945-1955.
38. Pogliaghi, M., M. Ripa, S. Pensieroso, M. Tolazzi, S. Chiappetta, S. Nozza, A. Lazzarin, G. Tambussi, and G. Scarlatti. 2015. Beneficial Effects of cART Initiated during Primary and Chronic HIV-1 Infection on Immunoglobulin-Expression of Memory B-Cell Subsets. *PloS one* 10: e0140435.
39. Gutzeit, C., G. Magri, and A. Cerutti. 2014. Intestinal IgA production and its role in host-microbe interaction. *Immunological reviews* 260: 76-85.
40. Peterson, D. A., N. P. McNulty, J. L. Guruge, and J. I. Gordon. 2007. IgA response to symbiotic bacteria as a mediator of gut homeostasis. *Cell host & microbe* 2: 328-339.
41. Somsouk, M., J. D. Estes, C. Deleage, R. M. Dunham, R. Albright, J. M. Inadomi, J. N. Martin, S. G. Deeks, J. M. McCune, and P. W. Hunt. 2015. Gut epithelial barrier and systemic inflammation during chronic HIV infection. *Aids* 29: 43-51.
42. Clayton, F., G. Snow, S. Reka, and D. P. Kotler. 1997. Selective depletion of rectal lamina propria rather than lymphoid aggregate CD4 lymphocytes in HIV infection. *Clinical and experimental immunology* 107: 288-292.
43. Zhang, Z. Q., D. R. Casimiro, W. A. Schleif, M. Chen, M. Citron, M. E. Davies, J. Burns, X. Liang, T. M. Fu, L. Handt, E. A. Emini, and J. W. Shiver. 2007. Early depletion of proliferating B cells of germinal center in rapidly progressive simian immunodeficiency virus infection. *Virology* 361: 455-464.
44. Lindner, C., I. Thomsen, B. Wahl, M. Ugur, M. K. Sethi, M. Friedrichsen, A. Smoczek, S. Ott, U. Baumann, S. Suerbaum, S. Schreiber, A. Bleich, V. Gaboriau-Routhiau, N. Cerf-Bensussan, H. Hazanov, R. Mehr, P. Boysen, P. Rosenstiel, and O. Pabst. 2015. Diversification of memory B cells drives the continuous adaptation of secretory antibodies to gut microbiota. *Nature immunology* 16: 880-888.
45. Hong, J. J., P. K. Amancha, K. Rogers, A. A. Ansari, and F. Villinger. 2012. Spatial alterations between CD4(+) T follicular helper, B, and CD8(+) T cells during simian immunodeficiency

virus infection: T/B cell homeostasis, activation, and potential mechanism for viral escape. *Journal of immunology* 188: 3247-3256.

46. Petrovas, C., T. Yamamoto, M. Y. Gerner, K. L. Boswell, K. Wloka, E. C. Smith, D. R. Ambrozak, N. G. Sandler, K. J. Timmer, X. Sun, L. Pan, A. Poholek, S. S. Rao, J. M. Brenchley, S. M. Alam, G. D. Tomaras, M. Roederer, D. C. Douek, R. A. Seder, R. N. Germain, E. K. Haddad, and R. A. Koup. 2012. CD4 T follicular helper cell dynamics during SIV infection. *The Journal of clinical investigation* 122: 3281-3294.
47. Allam, A., S. Majji, K. Peachman, L. Jagodzinski, J. Kim, S. Ratto-Kim, W. Wijayalath, M. Merbah, J. H. Kim, N. L. Michael, C. R. Alving, S. Casares, and M. Rao. 2015. TFH cells accumulate in mucosal tissues of humanized-DRAG mice and are highly permissive to HIV-1. *Scientific reports* 5: 10443.
48. Moukambi, F., H. Rabezanahary, V. Rodrigues, G. Racine, L. Robitaille, B. Krust, G. Andreani, C. Soundaramourty, R. Silvestre, M. Laforge, and J. Estaquier. 2015. Early Loss of Splenic Tfh Cells in SIV-Infected Rhesus Macaques. *PLoS pathogens* 11: e1005287.
49. Kubinak, J. L., C. Petersen, W. Z. Stephens, R. Soto, E. Bake, R. M. O'Connell, and J. L. Round. 2015. MyD88 signaling in T cells directs IgA-mediated control of the microbiota to promote health. *Cell host & microbe* 17: 153-163.
50. Lochner, M., C. Ohnmacht, L. Presley, P. Bruhns, M. Si-Tahar, S. Sawa, and G. Eberl. 2011. Microbiota-induced tertiary lymphoid tissues aggravate inflammatory disease in the absence of RORgamma t and LTi cells. *The Journal of experimental medicine* 208: 125-134.
51. Xu, H., X. Wang, N. Malam, A. A. Lackner, and R. S. Veazey. 2015. Persistent Simian Immunodeficiency Virus Infection Causes Ultimate Depletion of Follicular Th Cells in AIDS. *Journal of immunology* 195: 4351-4357.
52. Yamamoto, T., R. M. Lynch, R. Gautam, R. Matus-Nicodemos, S. D. Schmidt, K. L. Boswell, S. Darko, P. Wong, Z. Sheng, C. Petrovas, A. B. McDermott, R. A. Seder, B. F. Keele, L. Shapiro, D. C. Douek, Y. Nishimura, J. R. Mascola, M. A. Martin, and R. A. Koup. 2015. Quality and quantity of TFH cells are critical for broad antibody development in SHIVAD8 infection. *Science translational medicine* 7: 298ra120.
53. Havenar-Daughton, C., M. Lindqvist, A. Heit, J. E. Wu, S. M. Reiss, K. Kendric, S. Belanger, S. P. Kasturi, E. Landais, R. S. Akondy, H. M. McGuire, M. Bothwell, P. A. Vagefi, E. Scully, I. P. C. P. Investigators, G. D. Tomaras, M. M. Davis, P. Poignard, R. Ahmed, B. D. Walker, B. Pulendran, M. J. McElrath, D. E. Kaufmann, and S. Crotty. 2016. CXCL13 is a plasma biomarker of germinal center activity. *Proceedings of the National Academy of Sciences of the United States of America* 113: 2702-2707.
54. Havenar-Daughton, C., D. G. Carnathan, A. Torrents de la Pena, M. Pauthner, B. Briney, S. M. Reiss, J. S. Wood, K. Kaushik, M. J. van Gils, S. L. Rosales, P. van der Woude, M. Locci, K. M. Le, S. W. de Taeye, D. Sok, A. U. Mohammed, J. Huang, S. Gumber, A. Garcia, S. P. Kasturi, B. Pulendran, J. P. Moore, R. Ahmed, G. Seumois, D. R. Burton, R. W. Sanders, G. Silvestri, and S. Crotty. 2016. Direct Probing of Germinal Center Responses Reveals Immunological Features and Bottlenecks for Neutralizing Antibody Responses to HIV Env Trimer. *Cell reports* 17: 2195-2209.
55. Buranapraditkun, S., F. Pissani, J. E. Teigler, B. T. Schultz, G. Alter, M. Marovich, M. L. Robb, M. A. Eller, J. Martin, S. Deeks, N. L. Michael, and H. Streeck. 2017. Preservation of Peripheral T Follicular Helper Cell Function in HIV Controllers. *Journal of virology* 91.
56. Tomaras, G. D., N. L. Yates, P. Liu, L. Qin, G. G. Fouda, L. L. Chavez, A. C. Decamp, R. J. Parks, V. C. Ashley, J. T. Lucas, M. Cohen, J. Eron, C. B. Hicks, H. X. Liao, S. G. Self, G. Landucci, D. N. Forthal, K. J. Weinhold, B. F. Keele, B. H. Hahn, M. L. Greenberg, L. Morris, S. S. Karim, W. A. Blattner, D. C. Montefiori, G. M. Shaw, A. S. Perelson, and B. F. Haynes. 2008. Initial B-cell responses to transmitted human immunodeficiency virus type 1: virion-binding immunoglobulin M (IgM) and IgG antibodies followed by plasma anti-gp41 antibodies with ineffective control of initial viremia. *Journal of virology* 82: 12449-12463.

57. Trama, A. M., M. A. Moody, S. M. Alam, F. H. Jaeger, B. Lockwood, R. Parks, K. E. Lloyd, C. Stolarchuk, R. Scearce, A. Foulger, D. J. Marshall, J. F. Whitesides, T. L. Jeffries, Jr., K. Wiehe, L. Morris, B. Lambson, K. Soderberg, K. K. Hwang, G. D. Tomaras, N. Vandergrift, K. J. Jackson, K. M. Roskin, S. D. Boyd, T. B. Kepler, H. X. Liao, and B. F. Haynes. 2014. HIV-1 envelope gp41 antibodies can originate from terminal ileum B cells that share cross-reactivity with commensal bacteria. *Cell host & microbe* 16: 215-226.

58. Williams, W. B., H. X. Liao, M. A. Moody, T. B. Kepler, S. M. Alam, F. Gao, K. Wiehe, A. M. Trama, K. Jones, R. Zhang, H. Song, D. J. Marshall, J. F. Whitesides, K. Sawatzki, A. Hua, P. Liu, M. Z. Tay, K. E. Seaton, X. Shen, A. Foulger, K. E. Lloyd, R. Parks, J. Pollara, G. Ferrari, J. S. Yu, N. Vandergrift, D. C. Montefiori, M. E. Sobieszczyk, S. Hammer, S. Karuna, P. Gilbert, D. Grove, N. Grunenberg, M. J. McElrath, J. R. Mascola, R. A. Koup, L. Corey, G. J. Nabel, C. Morgan, G. Churchyard, J. Maenza, M. Keefer, B. S. Graham, L. R. Baden, G. D. Tomaras, and B. F. Haynes. 2015. HIV-1 VACCINES. Diversion of HIV-1 vaccine-induced immunity by gp41-microbiota cross-reactive antibodies. *Science* 349: aab1253.

59. Sender, R., S. Fuchs, and R. Milo. 2016. Revised Estimates for the Number of Human and Bacteria Cells in the Body. *PLoS biology* 14: e1002533.

60. Mouquet, H., and M. C. Nussenzweig. 2012. Polyreactive antibodies in adaptive immune responses to viruses. *Cellular and molecular life sciences : CMLS* 69: 1435-1445.

61. Haynes, B. F., J. Fleming, E. W. St Clair, H. Katinger, G. Stiegler, R. Kunert, J. Robinson, R. M. Scearce, K. Plonk, H. F. Staats, T. L. Ortel, H. X. Liao, and S. M. Alam. 2005. Cardiolipin polyspecific autoreactivity in two broadly neutralizing HIV-1 antibodies. *Science* 308: 1906-1908.

FIGURE LEGENDS

Figure 1. Early treatment of HIV-1-infected patients preserves the resting memory B-cells in the gut.

(A) Flow cytometry was used to assess the total number and frequency of $CD19^+$ cells from patients given combination antiretroviral therapy (cART) either early after transmission (e-ART, black squares) or later on, during the chronic phase of the disease (l-ART, grey squares) and from healthy HIV-1-negative controls (white squares). **(B)** Gut B-cell subpopulations identified by flow cytometry. **(C)** Frequencies of mature naive B cells (MN, $CD21^+$ $CD27^-$), resting memory B cells (RM, $CD21^+$ $CD27^+$), activated memory B cells (AM, $CD21^-$ $CD27^+$), and tissue-like memory B cells (TLM, $CD21^-$ $CD27^-$) within the $CD19^+$ $CD38^{low}$ $CD10^-$ mature B-cell population. Horizontal lines depict mean values. Kruskal-Wallis test: ns, nonsignificant; * $P<0.05$ and ** $P<0.01$

Figure 2. Early treatment of HIV-1-infected patients preserves the IgA / IgG-secreting cell ratio in the gut.

(A) Frequency of antibody-secreting cells (ASCs), i.e., plasmablasts/plasma cells, among total $CD19^+$ $CD10^-$ mature cells in the e-ART (black squares) and l-ART (grey squares) HIV-1-infected patients and healthy controls (white squares), evaluated by flow cytometry. **(B)** Concentrations of total IgGs and IgAs released spontaneously in the supernatant by mucosal ASCs from patients after 6 days of culture, evaluated by ELISA. Horizontal lines depict mean values. Kruskal-Wallis test: ns, nonsignificant; * $P<0.05$ and ** $P<0.01$. **(C)** B-cell clonality analysis of total mucosal B cells in early- and late-treated patients with HIV-1 infection. Total mucosal B-cell repertoire in the early-treated (e-ART, black lines) and late-treated (l-ART, grey lines) patients, studied by PCR. DNA extracted from frozen sections of rectal mucosa from HIV-1-infected patients was subjected to CDRH3 PCR amplification using VH- and JH-

primers, as detailed in Methods. Representative normal CDR3-size distribution of the polyclonal profiles in the e-ART and l-ART groups is shown. **(D)** Clonality profile of the mucosal B-cell repertoire from 3 e-ART and 1 l-ART patients showing small expanded clonal populations (arrows). **(E)** Dot plot comparing the mucosal B-cell repertoires of e-ART (n=12) and l-ART patients (n=12). The number of B-cell expansions in each group is shown in the top panel, where each symbol represents a donor. The frequency of patients harboring B-cell expansions is given in the pie charts (bottom panel); the number in the middle of each chart is the number of patients. The two-sided nonparametric Mann-Whitney U test.

Figure 3. Follicular helper T cells (T_{FH}) are expanded in the gut of early-treated HIV-1-infected patients.

(A) Gating strategy of mucosal T_{FH} cells (B) Frequencies of mucosal T_{FH} cells ($CXCR5^+$ $PD1^{high}$ $BCL6^+$) within the $CD3^+CD4^+$ T-cell population in the HIV-1-infected patients and healthy controls. Horizontal lines depict mean values. Kruskal-Wallis test: ns, nonsignificant; *P<0.05; **** P<0.0001. **(C)** Correlation between the frequencies of T_{FH} cells and RM B cells in the gut, assessed using Spearman's rank order test. **(D)** Blood circulating-T_{FH}-cell subpopulations identified by flow cytometry. **(E)** Frequency of total pre-T_{FH} cells ($CD3^+CD4^+CXCR5^+CCR7^-$) and frequencies of $CXCR3^+CCR6^-$ (c-T_{FH}1), $CXCR3^-CCR6^-$ (c-T_{FH}2), and $CXCR3^-CCR6^+$ (c-T_{FH}17) within the $CD3^+CD4^+CXCR5^+CCR7^-$ T-cell population. Horizontal lines depict mean values. Kruskal-Wallis test: ns, nonsignificant.

Figure 4. Lymphoid structures in the gut of early-treated patients are permissive for the maintenance of T_{FH} cells.

(A) Representative immunohistological stains for Pax5 (top panels) and PD-L1 (bottom panels) in rectal biopsies from patients given e-ART (n=6, left panels) or l-ART (n=6, right

820 panels). (B) The table lists the biopsies with and without PD-L1 expression (PD-L1$^+$ and PD-
821 L1$^-$, respectively). The asterisk indicates absence of co-localization between PD-L1 and Pax5
822 staining.
823
824 **Figure 5. HIV-1 Env gp140-reactive B cells are expanded in the gut of early-treated**
825 **HIV-1-infected patients and correlate with the frequency of gut-resident T_{FH} cells.**
826 **(A)** Representative dot plots of gp140-reactive mucosal B cells from healthy HIV-1-negative
827 controls (HIV$^-$) and HIV-1-infected patients (HIV$^+$). **(B)** and **(C)** Total mucosal HIV-1-
828 gp140-reactive CD19$^+$ cells: frequencies (B) and (C) distribution among the different B-cell
829 compartments. **(D)** B-cell receptor (BCR) isotypes expressed by the gp140-reactive resting
830 memory (RM) B cells in the e-ART and l-ART groups, compared using the two-sided
831 nonparametric Mann-Whitney U test: **P*<0.05. **(E)** Correlation between the frequencies of
832 mucosal T_{FH} cells and gp140-reactive CD19$^+$ cells in the gut, assessed using Spearman's rank
833 order test. **(F)** Reactivity against immobilized gp140 of total IgG (2 µg/mL) released by
834 mucosal ASCs, either spontaneously (without stimulation) or following *in vitro* differentiation
835 (IL-4, IL-21, and anti-CD40). The two-sided nonparametric Mann-Whitney U test was used:
836 ns, nonsignificant and **P*<0.05.
837
838 **Figure 6. Higher frequency of HIV-1-specific-IL21 secreting T cells in the blood of early-**
839 **treated patients.**
840 **(A)** and **(B)** The graphs depict the concentrations of IL-21 and IFN-γ released in the
841 supernatant by total peripheral blood mononuclear cells (PBMCs, $5{\cdot}10^5$ cells per well) from e-
842 ART and l-ART patients **(A)** after stimulation with *Staphylococcus aureus* endotoxin B
843 superantigen (SEB, 50 ng/mL) or **(B)** a pool of peptides derived from the HIV-1 Gag
844 polyprotein and HIV-1 Env glycoprotein gp160 (HIV-1 antigens, all 1 µg/mL), for 6 days.

Horizontal lines depict median values. Two-sided nonparametric Mann-Whitney U test: ns, nonsignificant and *P<0.05.

Supplemental Figure 1. **Early treatment of HIV-1-infected patients preserves resting memory B-cells in blood.** Frequencies of mature naive B cells (MN, CD21+ CD27-), resting memory B cells (RM, CD21+ CD27+), activated memory B cells (AM, CD21-CD27+), and tissue-like memory B cells (TLM, CD21- CD27-) among CD19+ CD38low CD10- mature B cells in the blood from early-treated patients (e-ART, blue squares) and late-treated patients (l-ART, red squares) and from healthy HIV-negative controls (HIV-, white squares).

Supplemental Figure 2. mRNA factors important for the germinal center's functions are higher in the gut of early-treated HIV-1-infected patients. (A) IL-6-, IL-27p28-, IL-27 EBI-3-, and IL-12A mRNA expressions in rectal biopsies of HIV-1-infected patients, quantified by qPCR. The histograms depict mean± SEM. The two-sided nonparametric Mann-Whitney U test was used: ns, non significant; *P<0.05 **(B)** AICDA mRNA transcripts in rectal biopsies from the patients, quantified by qPCR. Histograms depict mean values ± SEM. Kruskal-Wallis test: ns, non significant and **P<0.01.

Supplemental Figure 3. The frequency of gp140-reactive B cells is higher in the blood of early-treated HIV-1-infected patients.

Frequencies of total gp140-reactive CD19+ cells in the blood and gut of e-ART and l-ART patients. Two-sided nonparametric Mann- Whitney U test: *P<0.05.

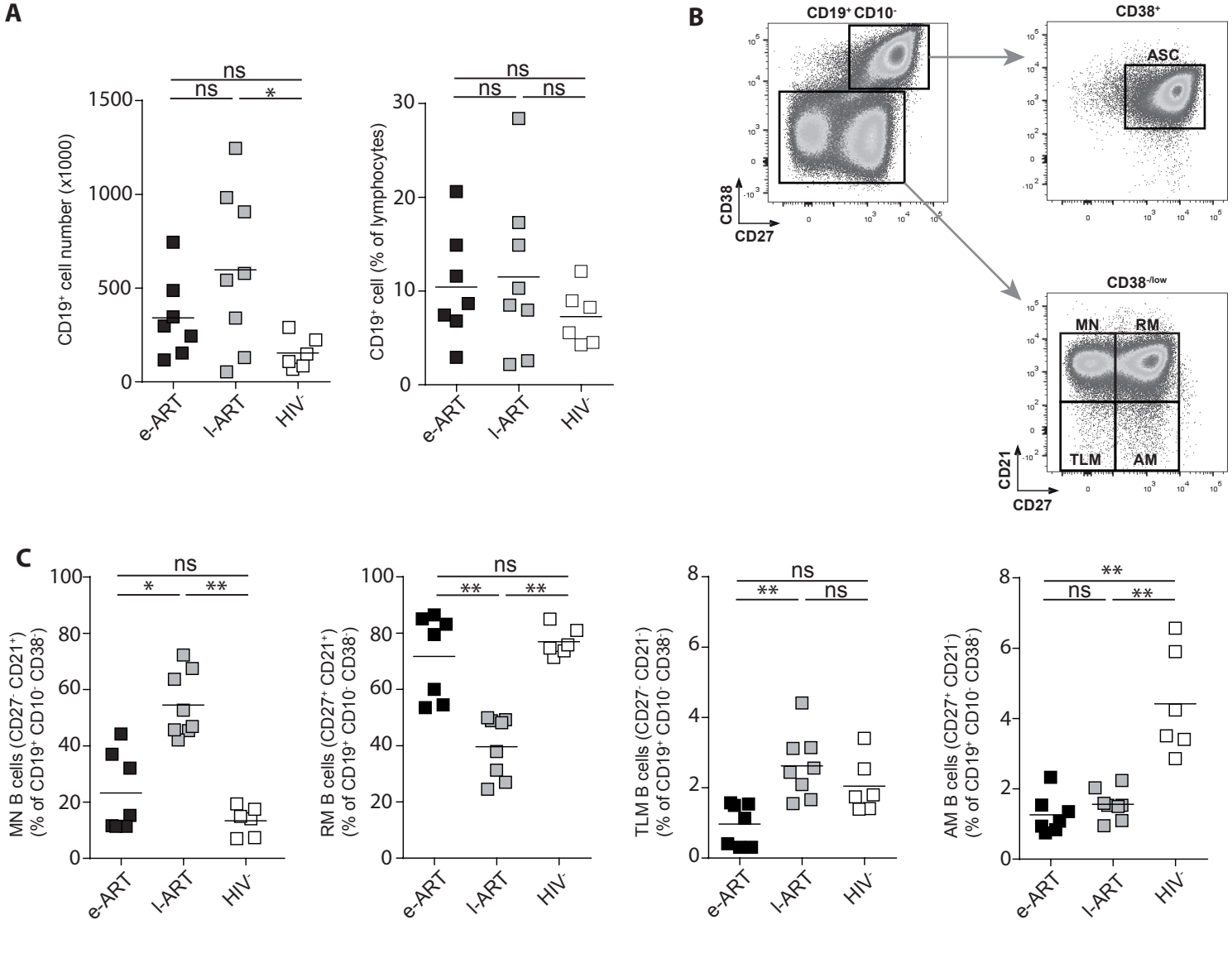
A
ns
ns
*
1500
1000
500
0
CD19+ cell number (x1000)
e-ART
I-ART
HIV-
ns
ns
ns
30
20
10
0
CD19+ cell (% of lymphocytes)
e-ART
I-ART
HIV-
B
CD19+ CD10-
CD38
CD27
CD38+
ASC
CD38-/low
MN
RM
TLM
AM
CD21
CD27
C
ns
*
**
100
80
60
40
20
0
MN B cells (CD27- CD21+) (% of CD19+ CD10- CD38-)
e-ART
I-ART
HIV-
ns
**
**
RM B cells (CD27+ CD21+) (% of CD19+ CD10- CD38-)
e-ART
I-ART
HIV-
ns
**
ns
8
6
4
2
0
TLM B cells (CD27- CD21-) (% of CD19+ CD10- CD38-)
e-ART
I-ART
HIV-
**
ns
**
AM B cells (CD27+ CD21-) (% of CD19+ CD10- CD38-)
e-ART
I-ART
HIV-

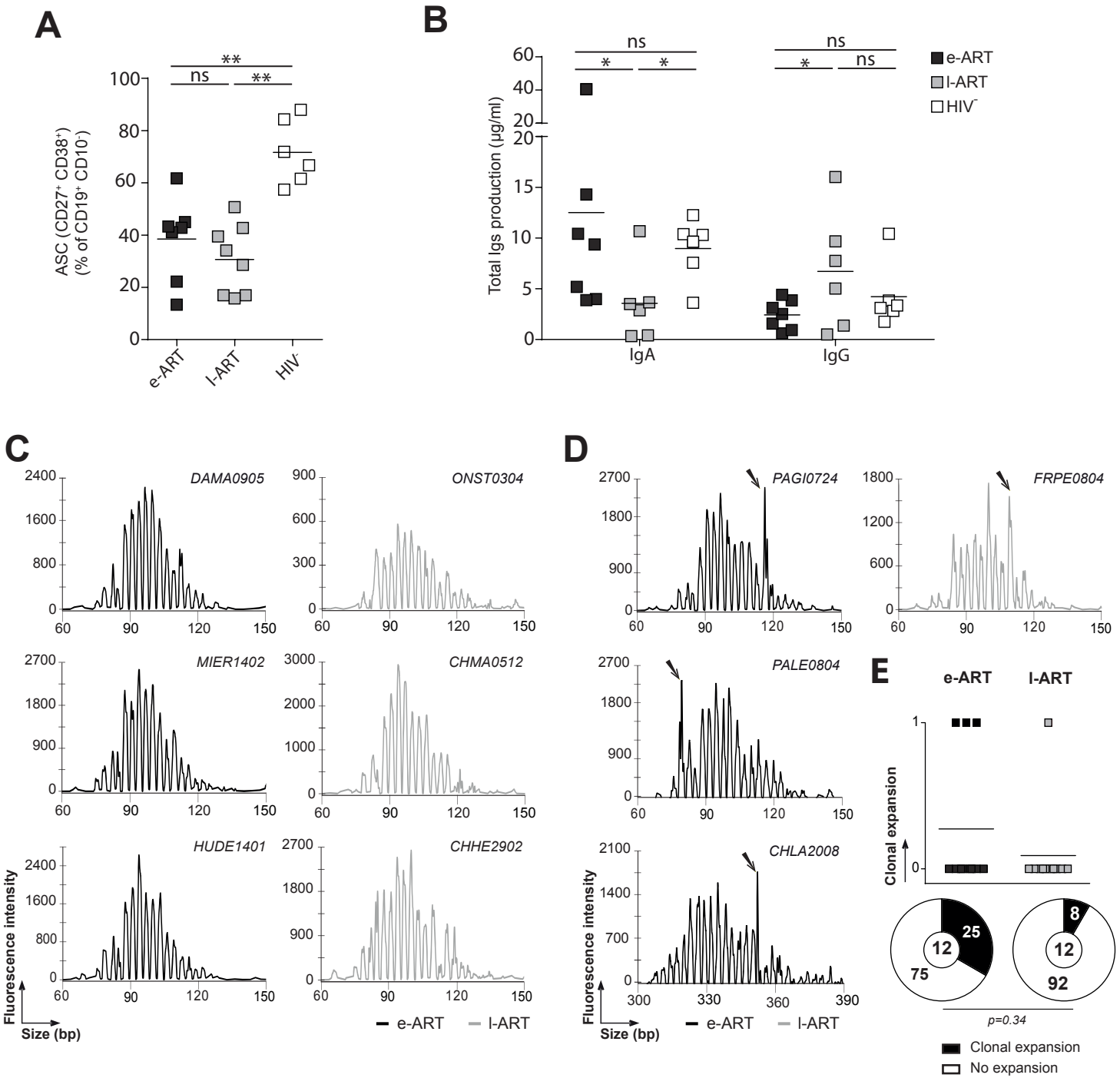
A
ASC (CD27+ CD38+) (% of CD19+ CD10-)
ns
**
**
e-ART
I-ART
HIV-
B
Total Igs production (µg/ml)
ns
ns
*
*
*
ns
IgA
IgG
e-ART
I-ART
HIV-
C
DAMA0905
ONST0304
MIER1402
CHMA0512
HUDE1401
CHHE2902
Fluorescence intensity
Size (bp)
e-ART
I-ART
D
PAGI0724
FRPE0804
PALE0804
CHLA2008
Fluorescence intensity
Size (bp)
e-ART
I-ART
E
e-ART
I-ART
Clonal expansion
25
12
75
8
12
92
p=0.34
Clonal expansion
No expansion

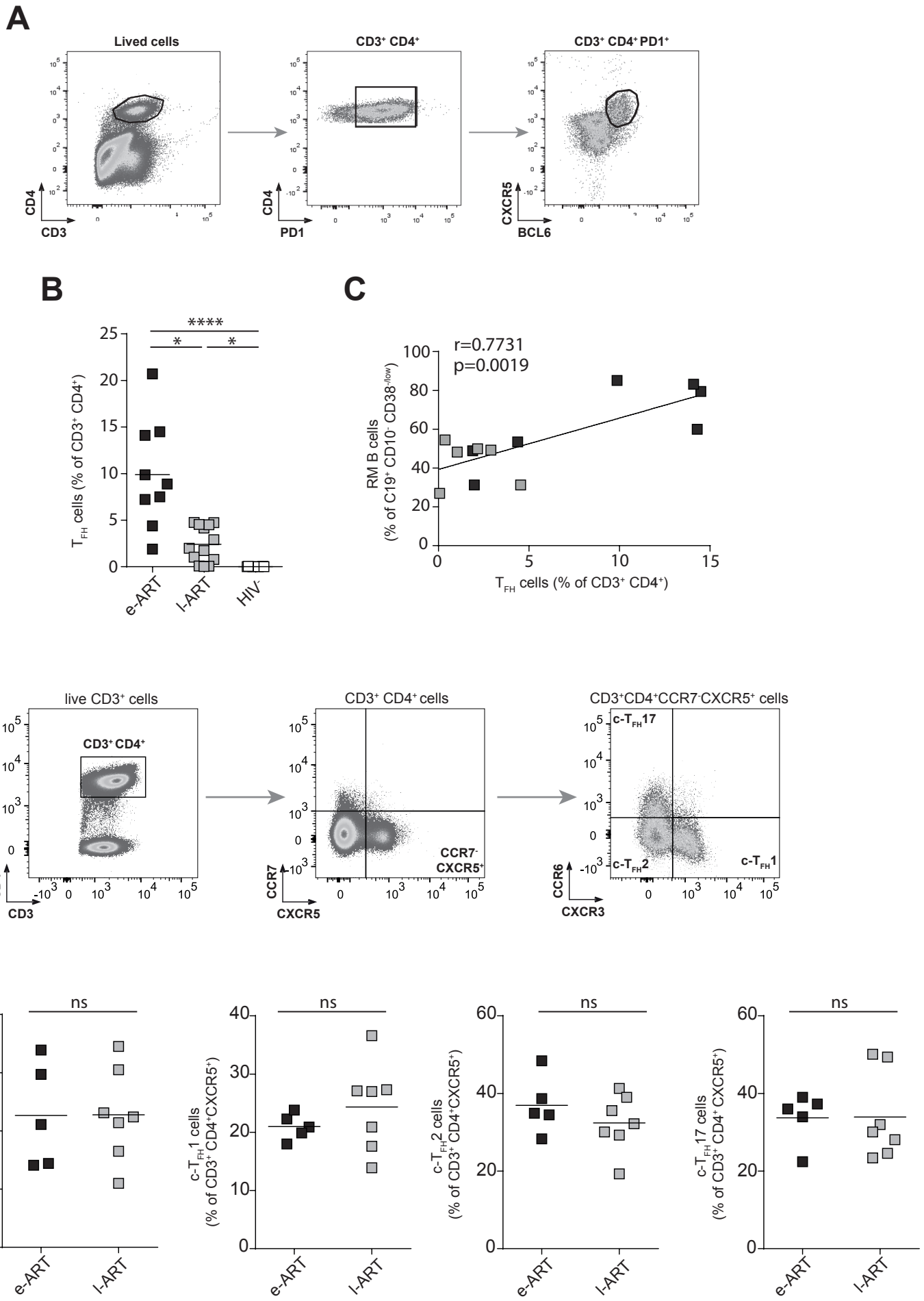
A
Lived cells
CD3+ CD4+
CD3+ CD4+ PD1+
CD4
CD3
CD4
PD1
CXCR5
BCL6
B
****
*
*
TFH cells (% of CD3+ CD4+)
e-ART
l-ART
HIV-
C
r=0.7731
p=0.0019
RM B cells
(% of C19+ CD10- CD38-/low)
TFH cells (% of CD3+ CD4+)
D
live CD3+ cells
CD3+ CD4+ cells
CD3+CD4+CCR7-CXCR5+ cells
CD3+ CD4+
CD4
CD3
CCR7-
CXCR5+
CCR7
CXCR5
c-TFH17
c-TFH2
c-TFH1
CCR6
CXCR3
E
ns
c-TFH cells
(% of CD3+ CD4+)
c-TFH1 cells
(% of CD3+ CD4+CXCR5+)
c-TFH2 cells
(% of CD3+ CD4+CXCR5+)
c-TFH17 cells
(% of CD3+ CD4+ CXCR5+)
e-ART
l-ART

A

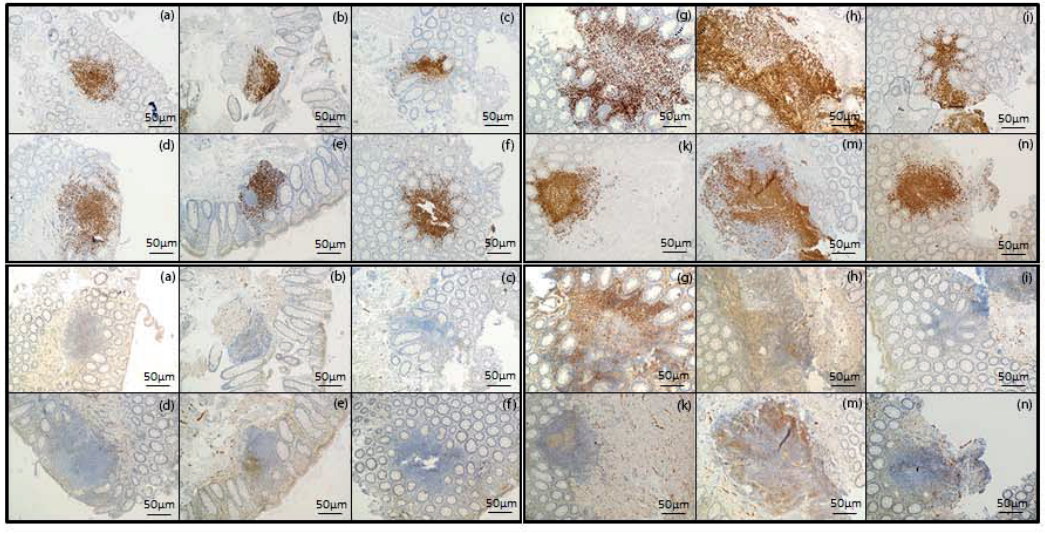

B

	Early cART	Late cART
	n=6	n=6
PD-L1$^-$	(a) (b) (c) (d) (f)	(i)
PD-L1$^+$	(e)*	(g) (h) (k) (m)* (n)*

*: PD-L1 staining not colocalized with Pax5 staining

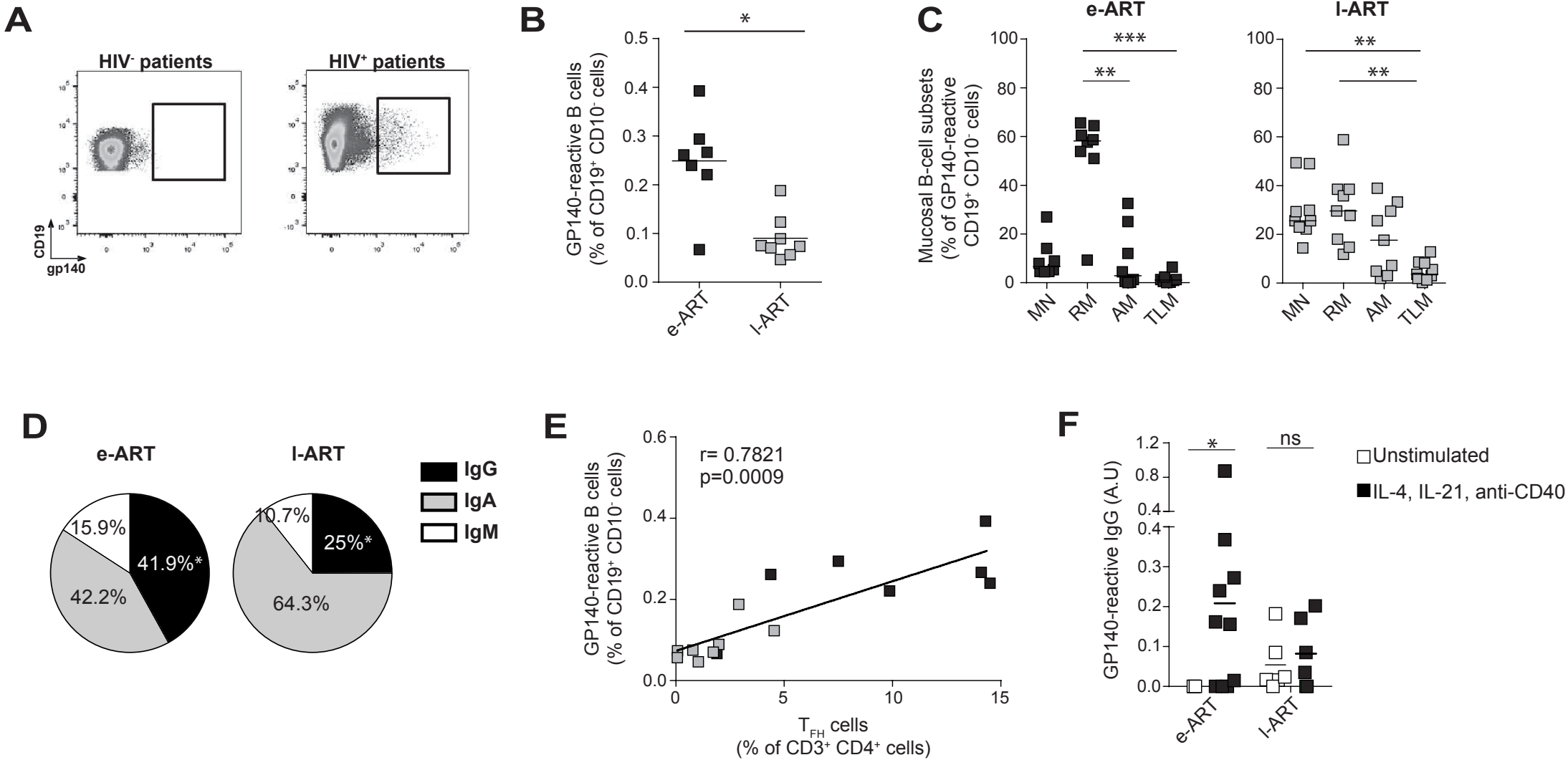
A
HIV- patients
HIV+ patients
CD19
gp140
B
GP140-reactive B cells
(% of CD19+ CD10- cells)
*
e-ART
l-ART
C
e-ART
l-ART
Mucosal B-cell subsets
(% of GP140-reactive
CD19+ CD10- cells)
***
**
MN
RM
AM
TLM
D
e-ART
l-ART
IgG
IgA
IgM
15.9%
41.9%*
42.2%
10.7%
25%*
64.3%
E
r= 0.7821
p=0.0009
GP140-reactive B cells
(% of CD19+ CD10- cells)
TFH cells
(% of CD3+ CD4+ cells)
F
GP140-reactive IgG (A.U)
ns
Unstimulated
IL-4, IL-21, anti-CD40

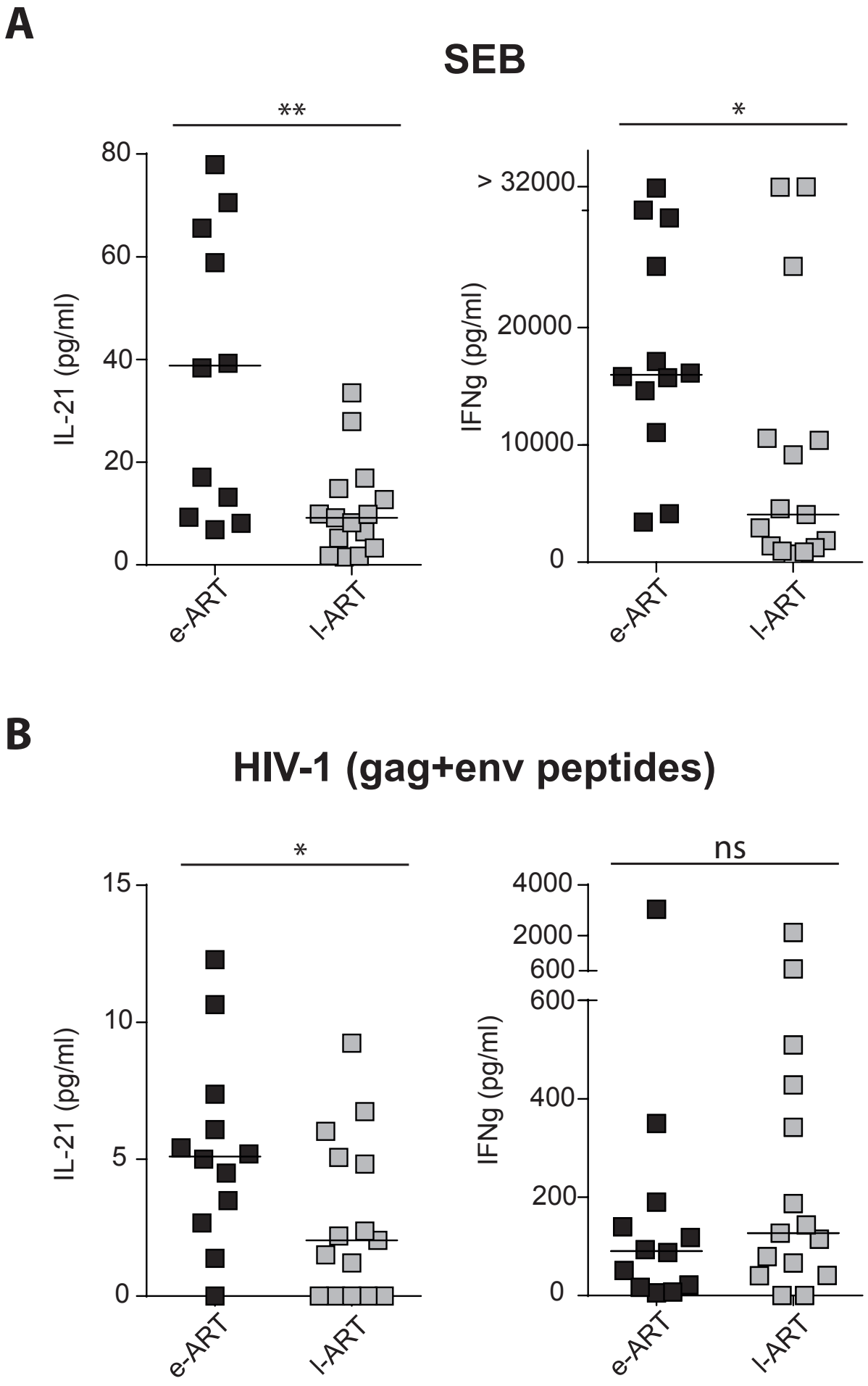
A
SEB
**
*
80
60
40
20
0
IL-21 (pg/ml)
> 32000
20000
10000
0
IFNg (pg/ml)
e-ART
l-ART
e-ART
l-ART
B
HIV-1 (gag+env peptides)
*
ns
15
10
5
0
IL-21 (pg/ml)
4000
2000
600
600
400
200
0
IFNg (pg/ml)
e-ART
l-ART
e-ART
l-ART

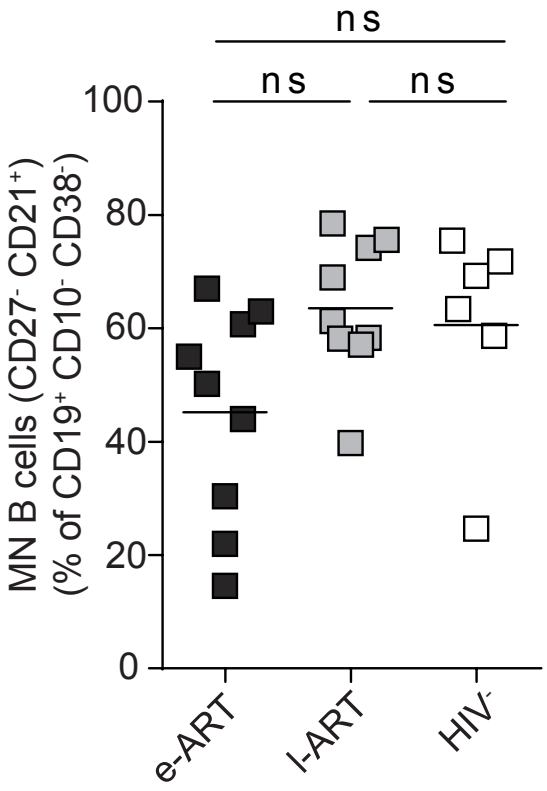
ns
ns
ns
MN B cells (CD27- CD21+)
(% of CD19+ CD10- CD38-)
100
80
60
40
20
0
e-ART
l-ART
HIV-

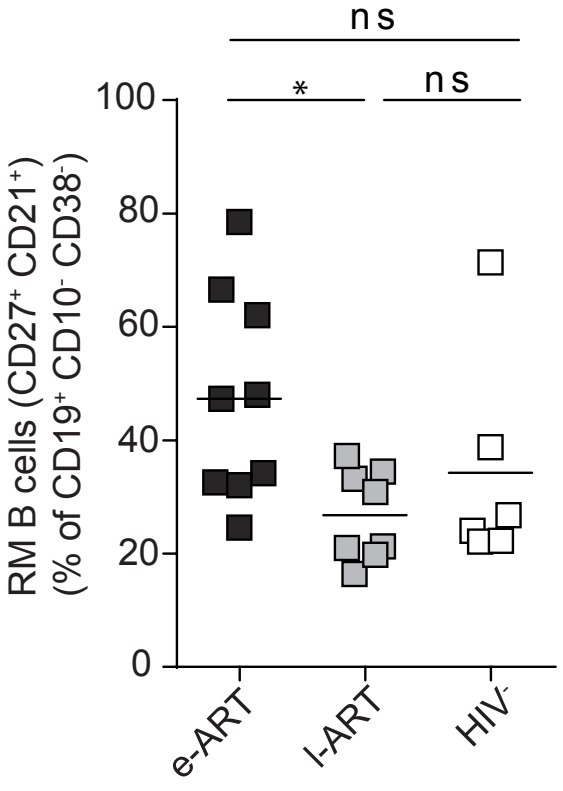
ns
*
ns
RM B cells (CD27+ CD21+)
(% of CD19+ CD10- CD38-)
100
80
60
40
20
0
e-ART
l-ART
HIV-

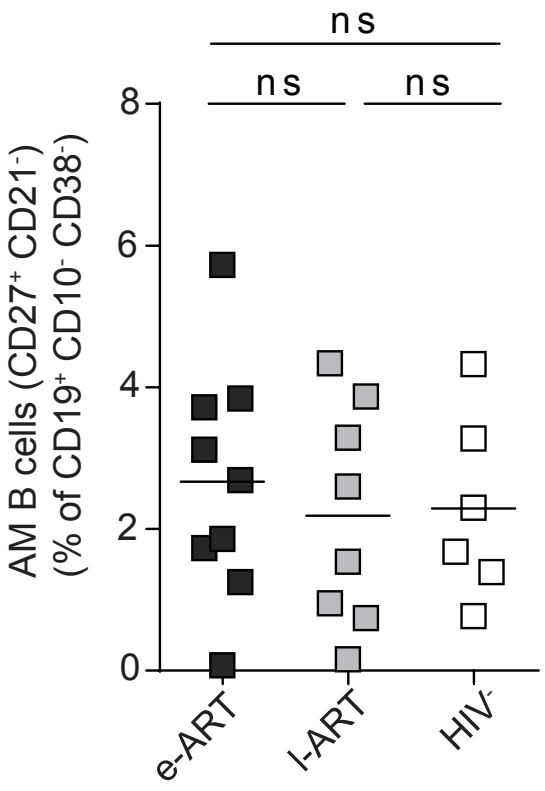
ns
ns
ns
AM B cells (CD27+ CD21-)
(% of CD19+ CD10- CD38-)
8
6
4
2
0
e-ART
l-ART
HIV-

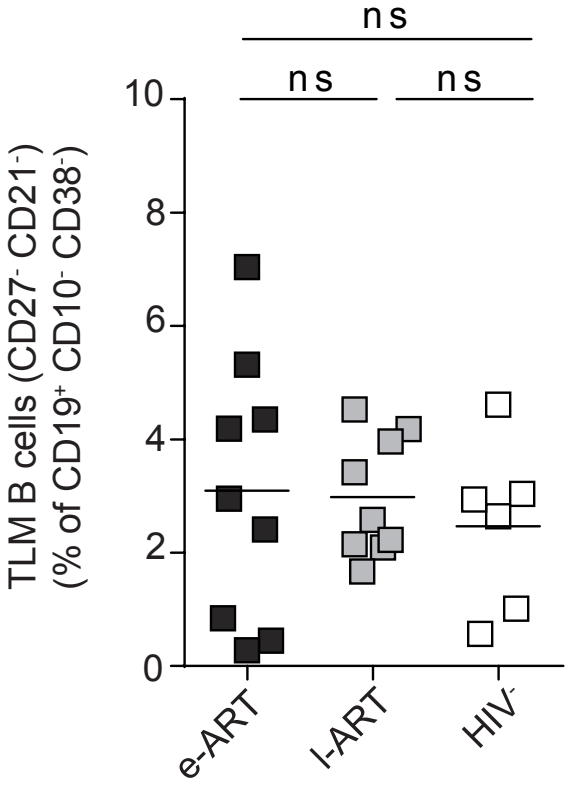
ns
ns
ns
TLM B cells (CD27- CD21-)
(% of CD19+ CD10- CD38-)
10
8
6
4
2
0
e-ART
l-ART
HIV-

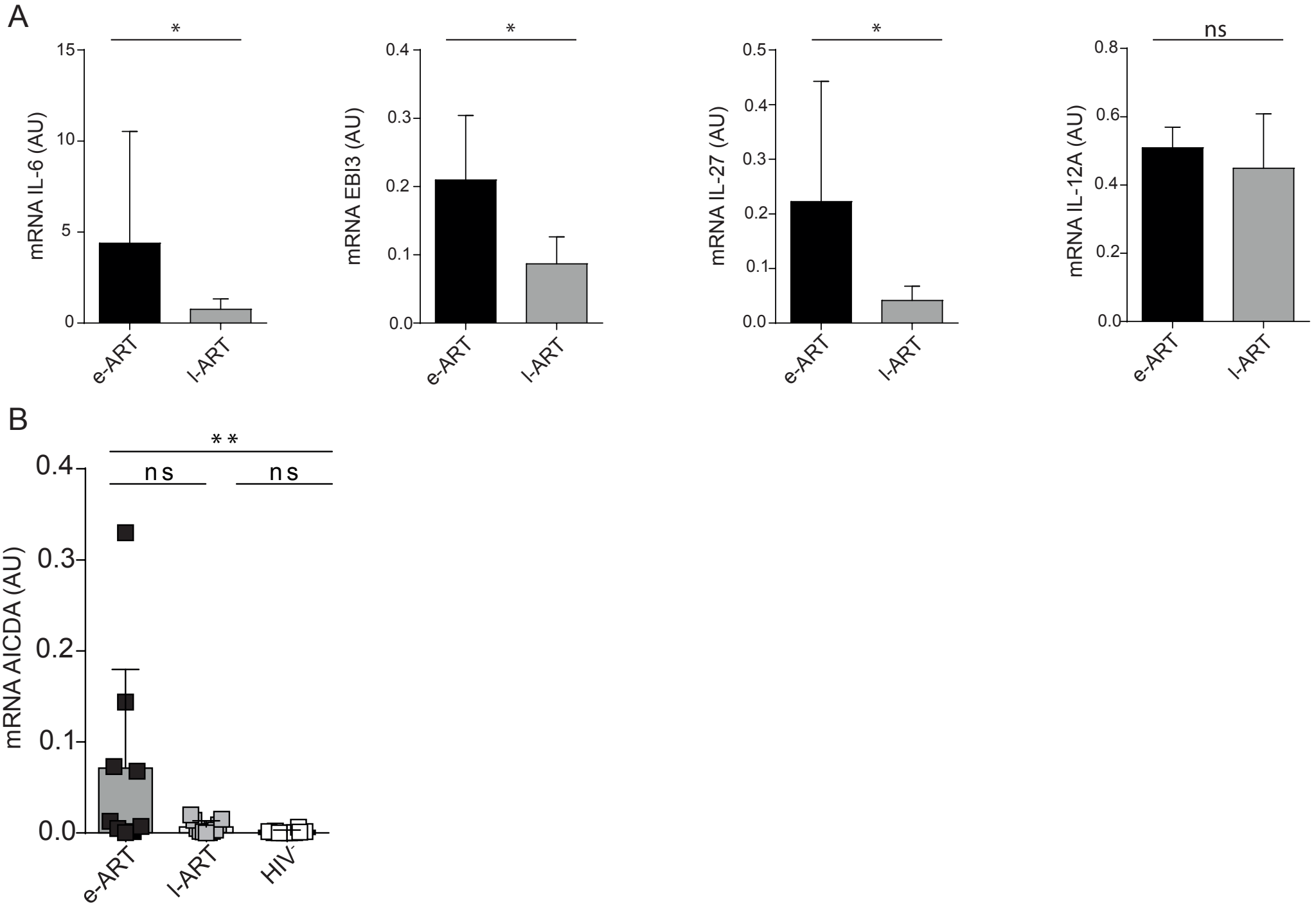
A
*
mRNA IL-6 (AU)
15
10
5
0
e-ART
l-ART
*
mRNA EBI3 (AU)
0.4
0.3
0.2
0.1
0.0
e-ART
l-ART
*
mRNA IL-27 (AU)
0.5
0.4
0.3
0.2
0.1
0.0
e-ART
l-ART
ns
mRNA IL-12A (AU)
0.8
0.6
0.4
0.2
0.0
e-ART
l-ART
B
**
ns
ns
mRNA AICDA (AU)
0.4
0.3
0.2
0.1
0.0
e-ART
l-ART
HIV-

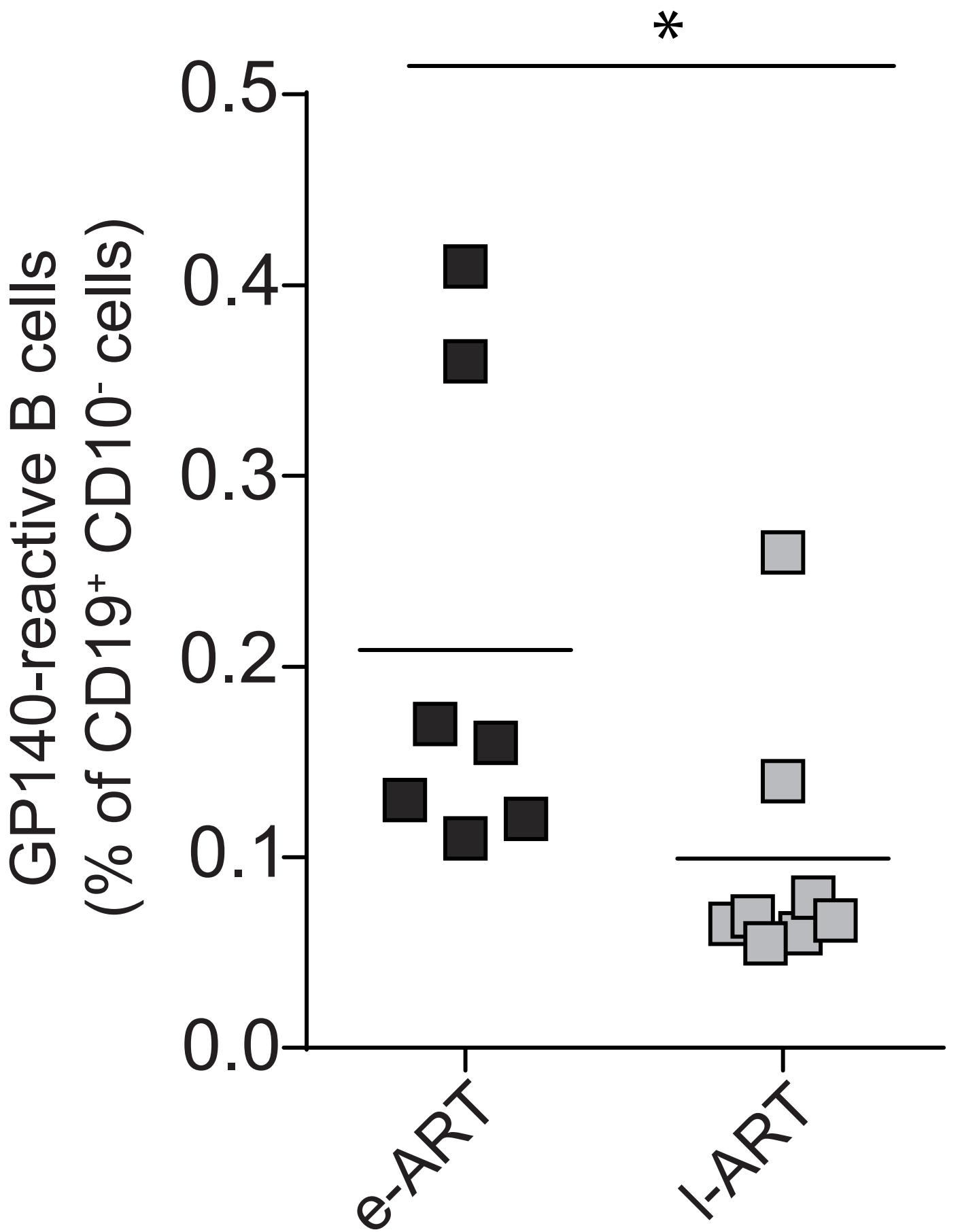
*
0.5
0.4
0.3
0.2
0.1
0.0
GP140-reactive B cells
(% of CD19+ CD10- cells)
e-ART
l-ART